AN EXPERIMENTAL STUDY

OF WIND RIPPLES

by

JAMES DOUGLAS WALKER

B. Sci. Geology
Massachusetts Institute of Technology
(1980)

SUBMITTED IN PARTIAL FULFILLMENT
OF THE REQUIREMENTS OF THE
DEGREE OF

MASTER OF SCIENCE IN
GEOLOGY

at the

MASSACHUSETTS INSTITUTE OF TECHNOLOGY

January 1981

Signature of Author_____
Department of Earth and Planetary Sciences
December 22, 1980

Certified by_____
J. B. Southard
Thesis Supervisor

Accepted by_____
Chairman, Department Committee

AN EXPERIMENTAL STUDY OF WIND RIPPLES

by

JAMES DOUGLAS WALKER

Submitted to the Department of Earth and Planetary Sciences on December 22, 1980 in partial fulfillment of the requirements for the Degree of Master of Science in Geology

ABSTRACT

Experiments were made on the effects of sediment size, sediment sorting, and wind velocity on morphology of eolian ripples. Several well sorted sands spanning the mean size range from 0.20 mm to 0.78 mm were selected to isolate the changes in ripple morphology with grain size. Further experiments were made using a poorly sorted sand to analyze the effect of sorting. A wind tunnel 30 m long, 0.6 m high, and 1.2 m wide was constructed for studying wind ripples and was used exclusively in this study.

Results from experiments made in well sorted sands show that ripple spacing and index increase with velocity, while ripple height decreases. Results from runs with poorly sorted sand show that for a given grain size ripple spacing increases as sorting becomes poorer. Previous assumptions regarding mechanisms controlling the variation of ripple morphology with grain size, sorting, and wind velocity are shown to be incomplete and only partially accurate.

Measurements of wind-velocity profiles indicate a greater-than-expected measured velocity in the saltation layer in comparison with the logarithmic wall law of the outer flow (flow above the saltation layer). Also shown is an increase in the shear stress borne by the fluid at the bed with increasing shear velocity of the outer flow.

Thesis Supervisor: Dr. John B. Southard

Title: Professor of Geology

TABLE OF CONTENTS

LIST OF SYMBOLS

A - Ripple asymmetry index

B - Bulk volume of sand

C - Inverse of von Karman's constant ($C = 1/0.40$)

C_1 - Inverse of von Karman's constant in sand-transporting flows ($C_1 = 1/0.375$)

C_f - Friction coefficient

c - Ripple speed

D - Mean grain size

G - Mass of sand in transport at a given time

G' - Mass of sand that ceases moving immediately after saltating

G'' - Mass of sand newly moved by the wind

g - Acceleration of gravity

H - Height of saltation layer

H_0 - Original bed height

h - Ripple height

h_0 - Perturbation height

I - Ripple index

I_β - Intensity of saltation at the bed

i - Impact-zone length and stoss-slope length

K - Roughness height in sand-transporting flows

k - Inverse of ripple spacing

L - Ripple spacing

m - Transport rate by creep over a flat surface

o - Center of area of a single ripple

q - Transport rate by creep

s - Shadow-zone length and lee-slope length

U - Mean flow velocity

U_c - Critical velocity for sand transport

U_{20} - Velocity at 20 cm above the bed

U_* - Shear velocity

α - Impact angle of saltating grains

β - Angle between ripple surface and horizontal

δ - Transport lag distance

μ - Fluid viscosity

ρ - Fluid density

ρ_s - Sediment density

σ - Sediment sorting

τ - Bed shear stress

FIGURES

ACKNOWLEDGEMENTS

Neither space nor time permits me to name and thank all of the people who in some way aided in the completion of this thesis, but without their help this work would have been quite difficult, if not impossible. For those I have omitted, I send my personal thanks.

I am especially grateful to Professor John B. Southard; without his support this project would have never been realized. His help in and out of both the classroom and laboratory was invaluable in developing my understanding of sediment transport and how it relates to geology.

I would also like to thank Kevin Bohacs and Bill Corea for their advice and help. They made many hot days easier to endure, and greatly eased many of the frustrations and problems associated with experimental sedimentology. I must extend special appreciation to Peter Vrolijk for his valued advice and companionship that accompanied every stage of this thesis. He provided support and push during those particularily difficult times when motivation and enthusiasm started to wane. I also am grateful to Chris Paola and his uncanny ability to relate physics to sediment transport.

Other people at MIT who supported my work and meddlings in geology deserve my deepest thanks. Gary Axen and all of the clones, Bill Brace, B.C. Burchfiel, Marilyn Copley, Roger Kuhnle, and Ana Silfer all contributed to my education and thesis work.

I must also thank those people who assisted with the experiments. The services of master craftsmen Bill Chesterson and Ed Insel were invaluable to the completion of the wind tunnel. These two and Kim Crocker, Gail Jarvis, and Jim Phelps helped during many of the runs.

The time I spent with Ralph Hunter and the other people at USGS provided me with an excellent taste of field sedimentology. Ralph's instruction on eolian processes and stratification gave me inspiration in completing this thesis.

Lastly, I must thank my parents James and Naomi Walker for the moral support they gave me. They provided the needed good words and understanding that got me through MIT.

Financial support for this project was provided by the MIT Undergraduate Research Opportunities Program, MIT Department of Earth and Planetary Sciences Student Research Funding Committee, American Association of Petroleum Geologists, Eloranta Fellowship program, and NSF grant 7919994 EAR awarded to John Southard.

INTRODUCTION

Statement of Problem and General Introduction

Wind ripples are a unique bed phase ubiquitous on subaerial exposures of sand: whether it be on the giant ergs of Africa, on coastal dunes of North America, or on stranded bar-tops of rivers, wind ripples are commonly encountered. Bed forms resembling wind ripples are found on Mars, attesting to the wide range of conditions in which ripples can form.

We could assume, correctly, that as such a common modern feature, eolian ripples are also an everyday feature in ancient deposits. While intact ripples are seldom preserved (and what bed form is?), ripple-drift stratification formed by ripple migration is common. Thus, a detailed understanding of ripple kinematics and morphology would be quite valuable in the interpretation of ancient eolian deposits. Previous studies of wind ripples have left many aspects of their behavior unexplored. Indeed, most studies to date have been field oriented, investigating morphologic properties of ripples after sand-transporting winds have ceased; only one study (Sharp, 1963) has dealt quantitatively with active ripples in the field, and only three studies (Zingg, 1952; Bagnold, 1954; and Seppala and Linde, 1978) have dealt specifically with ripple behavior experimentally in controlled laboratory conditions. This sort of laboratory study is precisely the aim of this thesis.

Basic Terminology

Wind ripples are downwind-migrating asymmetrical ridges of sand. A ripple has several identifiable parts: stoss and lee slope, crest, and trough (Figure 1). The angle between the ripple surface and the average plane of the depositional surface is typically between 4° and 10° for the stoss slope and between 8° and 30° for the lee slope. Noting that the crest has a highest point and the trough a lowest, we define the length of the stoss and lee slopes as the distance between the crest top and the upwind trough bottom, and the crest top and the downwind trough bottom, respectively. The ripple spacing is defined as the distance from trough to trough measured perpendicular to the ripple trend. We define the ripple height as the distance between the plane connecting succeeding troughs and the parallel plane containing the highest point of the crest.

Sand movement in wind occurs in three modes: saltation, suspension, and surface creep. Sand transported in saltation moves in jumps over the sediment surface, travelling downwind typically tens to hundreds of grain diameters and rising tens of grain diameters. Sand moving in suspension never or rarely contacts the bed. Grains transported as surface creep roll along the bed surface rarely losing contact with other grains.

Conditions for Ripples

Wind ripples form in most sizes of sand. The lower

Figure 1. Morphologic features of wind ripples.

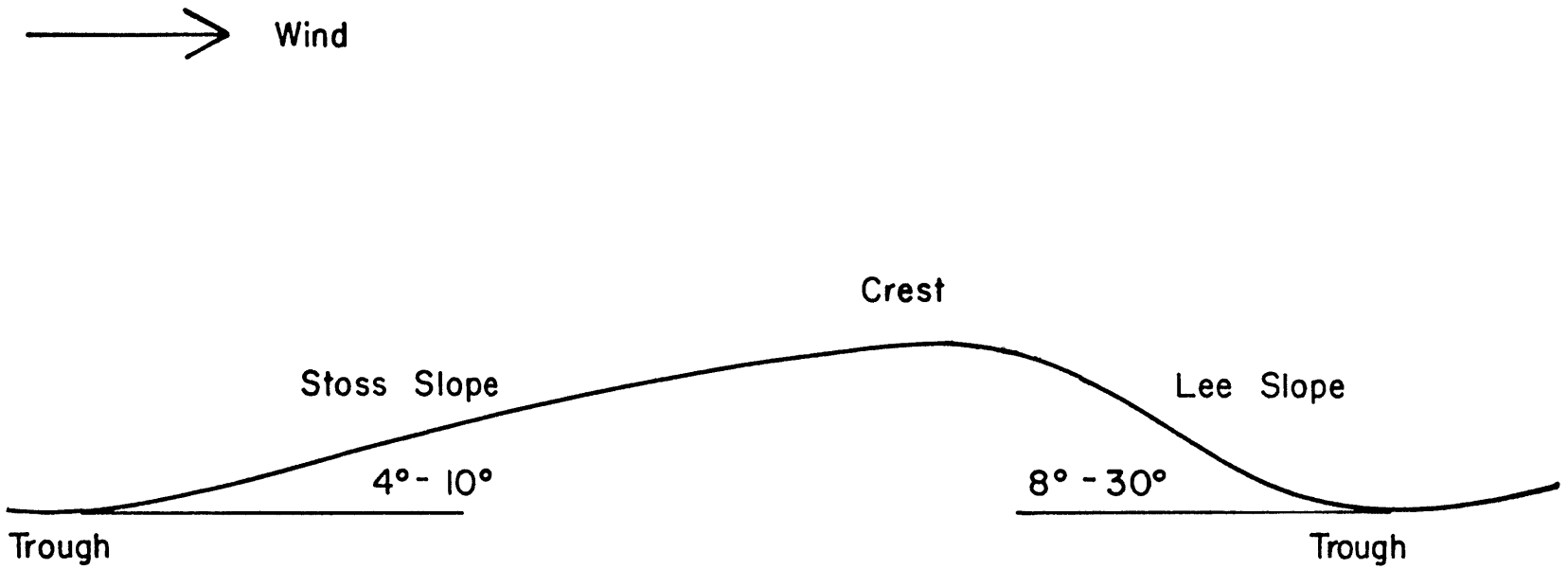
Wind
Crest
Stoss Slope
Lee Slope
4° - 10°
8° - 30°
Trough
Trough

limit of grain size seems to be governed by electrostatic grain-to-grain forces, which cause a sediment mixture to have such a high threshold for movement that eroded grains are immediately carried into suspension. The upper limit of grain size in which ripples can form is unknown (Figure 2). In fact, there may be no upper limit provided that the flow strength is sufficient to move the grains and that the grains do not self-destruct during transport. Wind velocity is also important, because ripples are not stable under every wind regime: velocity must be strong enough to transport sediment, but not so strong as to cause flat-bed transport. Sand sorting also affects whether ripples will form. Bagnold (1954) notes several sand mixtures in which ripples do not form. These are typically bimodal sands in which there is a 6-to-1 ratio of the modal sizes. Stone and Summers (1972) observed that particles of high density, but not radically different size, can inhibit ripple formation when introduced into the sediment mixture, demonstrating that ripple stability can also be affected by grain composition, heavy minerals for example.

But given favorable conditions wind ripples do form. Ripple behavior must be controlled by the factors governing these favorable conditions: characteristics of wind velocity and sediment size and sorting are important.

Review of Literature

Ripple morphology viewed as the interaction of

Figure 2. Possible field for ripples. Grains are assumed to be transported in suspension if the shear velocity is greater than the fall velocity.

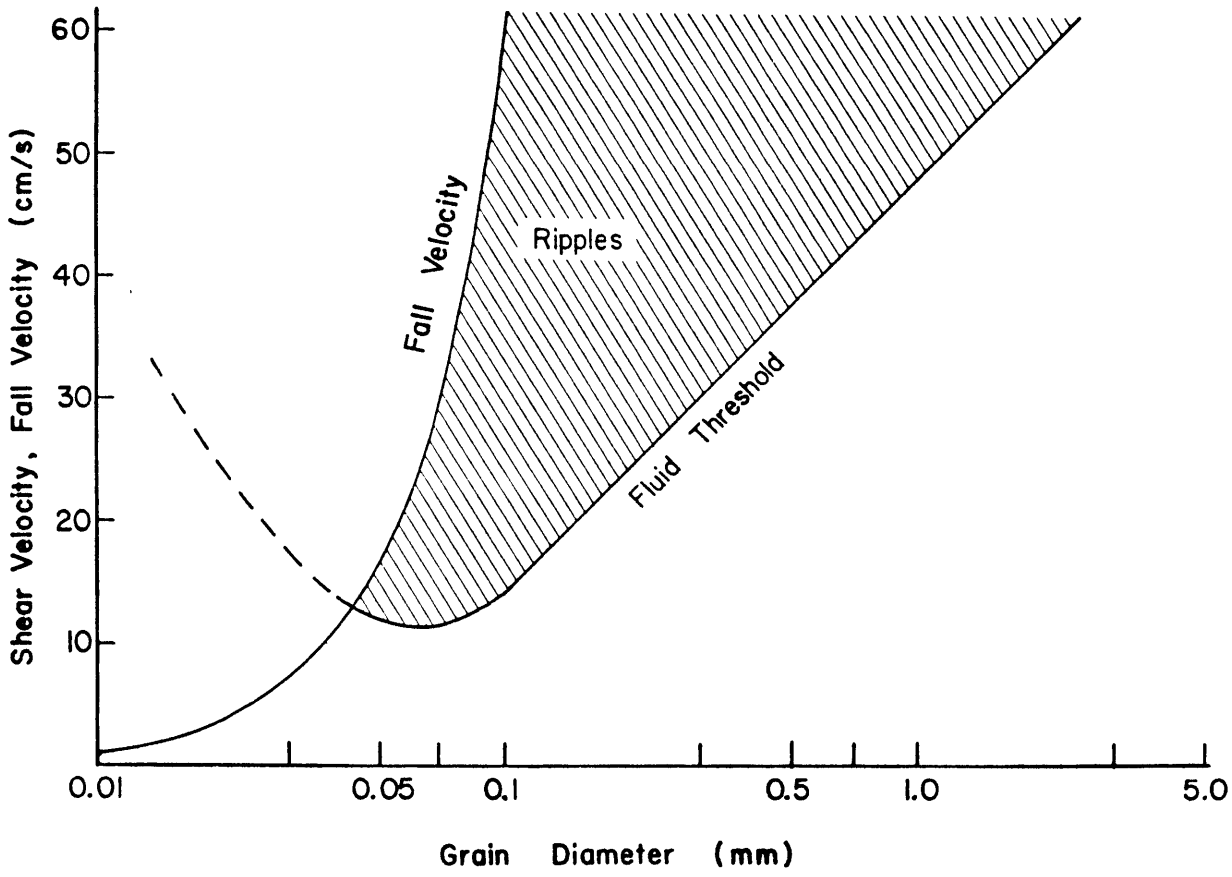
60
50
40
30
20
10
Shear Velocity, Fall Velocity (cm/s)
Fall Velocity
Ripples
Fluid Threshold
0.01
0.05
0.1
0.5
1.0
5.0
Grain Diameter (mm)

sedimentological and environmental factors started with Cornish and his classic work Waves of Sand and Snow (1914). Cornish made the first attempts at describing the modes of sediment transport by wind and the development of ripples from an initially flat bed; he noted the difference between saltation and surface creep, and he stated that ripples grow from small mounds which form on a flat sediment surface when transport begins. Cornish also made the first experiments on wind ripples, that resulted in the recognition that ripples are composed primarily of coarse sand moving on a surface of fines. However, he did not attempt to elucidate any of the controls exerted by sediment texture on ripple morphology.

Chepil (1945) made experiments on wind ripples and their effect on the roughness height in a wall-law equation. He found that ripples formed in soil particles with a mean diameter between 0.05 mm and 0.70 mm, but did not develop outside of this range. Chepil's study, however, was aimed not at wind ripples but surface roughness. Data of other workers contradict the 0.70 mm upper limit for ripple formation. Irregularities in Chepil's work may result from the fact that (1) his tunnel was only 4 m long; and (2) he used soil particles rather than quartz sand. Also, we do not know the exact nature of the particles used or the tunnel geometry or type (blower or suction).

Bagnold made many conceptual and experimental studies of wind ripples. We can summarize his findings as follows

(based on Bagnold, 1954): ripple spacing is equal to the length of the characteristic path of saltating grains, and height and index depend on sediment sorting.

Bagnold defines the characteristic path as that path which is equivalent to the average grain path in its effect on the wind. In other words, if every saltating grain moved according to the characteristic path, the wind profile would be the same as when grains saltated naturally. In turbulent flows mean velocity varies as the logarithm of the height above the bed, but when sediment-transporting flows are considered this is not strictly true (near the bed): velocity defects occur and are manifested as kinks in a semilog plot of velocity versus height. Bagnold assumed that these kinks mark the average height of saltating grains. In experiments in well sorted sand, with mean grain size between 0.18 mm and 0.30 mm, Bagnold found good agreement between the length of the characteristic path as computed from the kink height and the ripple spacing. Unfortunately, Bagnold simply states that the characteristic path can be computed mathematically without giving any details on how he computed it.

Bagnold gives five factors which govern ripple height, spacing, and shape:

1) wind which promotes saltation;

2) saltation which moves the surface creep;

3) surface grains which move both horizontally and vertically according to individual size,

shape, and density;

4) resulting surface relief which causes spatial variation in the ejection rates of grains due to the angle between the impacting grains and the sand surface; and

5) state of sand flux: steady, erosional, or depositional.

Bagnold viewed ejection rate of saltating grains and surface creep in the following way. If we return to the concept of characteristic path, saltating grains will impinge on the surface at an angle α to horizontal, the sand surface making an angle β with horizontal. Bagnold gives the following formulas:

$$I_\beta = \frac{\tan\alpha - \tan\beta}{\tan\alpha} * \frac{\cos(\alpha - \beta)}{\sec\beta}$$

or for most cases:

$$I_\beta = 1 - \frac{\tan\beta}{\tan\alpha} \qquad \{ \frac{\cos(\alpha - \beta)}{\sec\beta} \simeq 1, \text{ small } \alpha, \beta \}$$

where

I_β = relative intensity of saltating grains in propelling the surface creep

$I_\beta = 1$ for $\beta = 0$, the standard state being a horizontal surface. On stoss slopes $\beta<0$, so $I_\beta>1$, and on lee slopes $\beta>0$, so $I_\beta<1$. This explains why a horizontal surface is unstable: any surface relief will cause a variation in the surface creep, and this will create ripples. This also

explains why ripples migrate downwind: the stoss slopes are propelled past the lee. The rate of transport of surface grains depends on their physical properties (size, shape, density), creating sorting horizontally by differences in transport velocities and vertically by material stacking properties.

We may now view ripple spacing, height, and shape as a combination of the above five factors, and we will assume a steady sand flux. As stated above, ripple spacing is equal to the length of the characteristic grain path and thus primarily a function of wind velocity and its effect on the saltation profile.

Bagnold contends that ripple height depends on sorting of the sediment and believes that this is shown by differences between ripples in well sorted and poorly sorted sand. Ripples formed in well sorted sands tend to have low relief, resulting in large values of ripple index I (ratio of spacing to height), up to 70. In well sorted sands it is easier for saltating grains to move grains on the ripple crest, thus planing off the crest and reducing the height. Ripples formed in poorly sorted sand have lower values of ripple index, down to 10. Because of vertical sorting of sediment, ripple crests are composed of coarser grains, so saltating grains, on the average smaller than the grains at crests, do not move the crestal grains as easily, allowing the ripple to build higher.

Bagnold also describes why ripples form transverse to the

wind. If the ripple is concave upwind the horns move faster: the sand in creep is deflected towards the transverse portion, accelerating the horns. By similar reasoning, if the ripple is convex upwind the horns are slowed.

Theodore von Karman (1947) approached the problem of wind ripples from the standpoint of fluid mechanics. He assumed that because the crest is higher the flow there is moving faster, and thus the crest should tend to be planed off unless there is some opposing effect. Since grains are entrained in the flow, gravity acting on them accelerates the grains, and thus the flow, down the lee slope and thereby equalizes the velocity over the ripple. Von Karman deduced the following result for ripple spacing:

$$L = 2\pi U_g \sqrt{H/g}$$

where

L = the ripple spacing

H = the width of the heavy saltation stream

U_g = the velocity near the ground (von Karman does not specify this wind velocity any further)

g = the acceleration of gravity

Assuming that H is proportional to V_t^2/g, where V_t is the rms fluctuation of the vertical wind velocity component, we can write:

$$L = 2\pi U_g (V_t/g)$$

Assuming further that V_t is of the order $U_g\sqrt{C_f}$, where C_f is the friction coefficient, $C_f = \tau/(\rho U_g^2/2)$, τ is the bed shear stress and ρ is the density of air, we can write:

$$L = 2\pi U_g/\sqrt{C_f}$$

or about the same as the distance travelled by saltating grains (see von Karman, 1947).

But this is only an approximate solution, since a continuous stratification is present over the distance H and not a simple heavy stream. Furthermore, there is good evidence that the friction coefficient is approximately constant in sand-transporting flow, since shear velocity is a linear function of the mean velocity at a given height (Belly, 1964). Also the premise that ripples would be planed off is in doubt because ripples migrate downwind as a result of the higher velocity over the crest (?). Von Karman's is the only paper in the literature that deals with ripple spacing as a density stratification problem, though such an approach might have great potential.

The first extensive experimental study of wind ripples was made by Zingg (1952) in an unpublished Master's thesis. Zingg worked primarily with well sorted sand. The sands used were sieved to lie in the intervals 0.15 - 0.25 mm, 0.25 - 0.30 mm, 0.30 - 0.42 mm, 0.42 - 0.59 mm, and 0.59 - 0.84 mm. A naturally sorted Colorado dune sand was also studied. While the primary concern of Zingg's work was to investigate sand transport by wind (threshold velocity,

sand flux, etc.), he recognized the importance of ripples and presented data on their morphology.

Zingg found that for a given well sorted sand, ripple spacing and height increased with increasing bed shear stress, and in such a way that ripple index remains constant. He found the following relationship for I:

$$I = 75D^{3/4}$$

where

D = grain size in millimeters (this equation is not dimensionally balanced)

Unfortunately, Zingg never mentions whether flat-bed conditions were obtained. The rate of increase with shear stress varies among sands, but a marked difference is seen between the 0.25 - 0.30 mm size and 0.30 - 0.42 mm size: in the finer sands spacing increases smoothly with shear stress, but in sands coarser than 0.30 - 0.42 mm spacing increases smoothly to a certain point but then increases more rapidly. This inflection is manifested physically in the ripples: the ripples become disorganized and mottled in appearance. An especially interesting result obtained by Zingg is that ripple spacing is typically greater in finer sands and decreases with increasing sand size for a given shear stress.

The experiments using Colorado dune sand show many of the differences between naturally sorted and extremely well sorted sand. Experiments were made under conditions of net

erosion of the bed, with results plotted as spacing versus percentage of sand greater than 0.42 mm in diameter in the crest, contoured for shear stress. When these data are replotted at a constant crest-size content an interesting behavior is observed: sand with a low percentage of material greater than 0.42 mm is similar to finer sands in its variation of ripple spacing with shear stress, while sands greater in crest grain size behave like coarser sands. We can also note that ripple spacing increases with percentage of crestal grains above 0.42 mm (and thus mean grain size), whereas in well sorted sands spacing decreases with increasing grain size.

In summary, in well sorted sands ripple spacing increases with increasing shear stress and decreases with grain size, while in naturally sorted sands spacing increases with both shear stress and grain size.

The work of Sharp (1963) is the most complete field study of wind ripples and provides interesting insights into interpreting ripple behavior. His study, conducted on the Kelso dunes of the Mojave Desert, dealt primarily with internal ripple structure and ripple-drift deposits.

Sharp investigated internal structure by sectioning ripples that had been impregnated with plastic. He found that ripples consist of coarser ridges on a base of fine sand. While the crest is indeed coarse material, this coarseness actually represents an increase in the abundance of coarse grains and not an increase in their size. Finer

grains underlie the ripple and are seen in the trough and as a thin veneer up the stoss slope. When ripples are active, finer grains propel the material on the stoss slope over the crest by the action of saltation impact, and this results in ripple movement. Sharp observed that the sand composing the ripple is not representative of the dune sand as a whole: it is a mantle of coarser grains over normal dune sand. The sand below the ripple typically forms a thin "carpet" of finer grains, finer than the normal dune sand. Sharp proposed two possible mechanisms for producing this carpet: (1) it represents the erosional limit reached by the ripples, or (2) it represents deposition by the ripples by winnowing of the fine grains from the coarse as the ripple migrates. Sharp favored the latter explanation.

Sharp presented an elegant analysis of factors affecting morphology of ripples. The ripple has a height h, a spacing that is composed of an impact zone (stoss slope) i and a shadow zone (lee slope) s, and the saltating grains impinge at a characteristic angle α. According to Sharp, s depends directly on h and inversely on α. Also, h increases directly with the grain size D, and thus s increases with D. The impact angle varies inversely with wind velocity, so s varies directly with velocity. The only unknown relationship is between h and velocity. We know that h initially increases with velocity , but must eventually decrease, so the relationship is uncertain. Therefore, the exact dependence of s on velocity is unclear; the question remaining

is which dominates, α or h.

The impact zone i also depends on h and α. Like s, i increases with h, but the dependence on α is unclear. Sharp postulated that in a balanced system inclination of i varies inversely with both D and α, and directly with the impact energy of saltating grains. If the slope of i increases, then i increases. If D increases, so does i, and i decreases with impact energy, so i decreases with velocity.

From the reasoning above, Sharp concludes that if D increases, so must i and s, and thus also the ripple spacing. Since ripple spacing increases with velocity, s in fact increases with velocity, and does so faster than i decreases. Therefore, Sharp concluded that no relationship between Bagnold's characteristic path and ripple spacing is required or implied. Sharp also concluded that the ratio i/s increases with increasing D and decreases with increasing velocity, and this is what is observed in the field.

Kennedy (1963) analyzed wind ripples as a stability problem. One of his basic arguments is that a transport lag distance exists, that is, a finite distance between the point where the flow is perturbed by the ripple and the point where the sediment transport rate has responded to the perturbation. Kennedy assumed that transport rate is proportional to the ripple height and used empirical transport formulas (using a potential-flow law over the ripple) to derive values for ripple spacing, speed, and index:

$$L = 1.24\delta$$

$$c = \frac{n\langle G\rangle kU}{B(U-U_c)}$$

$$I = \frac{nU\pi}{b(U-U_c)}$$

where

δ = transport lag distance

n = exponent in the transport equation

$\langle G\rangle$ = mean transport rate

k = 1/L

U = free stream velocity

B = bulk volume of sand

b = ratio of total transport to creep

This analysis relies heavily on the existence of a lag distance. Kennedy cites Bagnold (1954) on this point: but Bagnold's data do not show a lag after transport is fully developed, and his sampling interval was 0.6 m, much longer than a typical ripple spacing. Kennedy states that at equilibrium the lag distance is equal to the ripple spacing, but this is not what his equations indicate. Therefore, serious problems are seen in the concept of a lag distance: few data (if any) support this idea.

Stone and Summers (1972) presented data on ripple morphology and the characteristics of the natural wind. Their findings can be summarized by the following quotation:

Wavelength increases until equilibrium is reached

> for that mean grain size and does not increase thereafter even though the wind velocity might increase.

In support of this statement they present a log-log plot of mean grain size versus ripple spacing. After several smoothings the plot yields the following relation:

$$L = 63.8D^{-0.75}$$

Stone and Summers explained that other authors failed to discover this relationship because (1) sampling error was present in either method or location on the ripple for sampling; (2) grain size studied was too small (Stone and Summers collected data over the range of 0.15 mm to 3.0 mm); and (3) insufficient time was allowed for ripples to reach equilibrium. Stone and Summers believed that ripple spacing is a function of grain size only.

Following the work of Wilson (1972), Ellwood, Evans, and Wilson (1975) recognized two types of ripples: impact ripples, which form in fine unimodal sand and have spacings from 1 cm to 20 cm; and megaripples, which form in coarse bimodal sand and have spacings between 20 cm and 25 m. The dynamic criterion used for distinguishing the two ripple types is based on the transport mode of the coarser grain sizes. In impact ripples coarse grains move in both saltation and creep, while in megaripples the coarse fraction moves solely as creep under the bombardment of the finer fraction. Because of this difference Ellwood *et al.* believed that

some sort of discontinuity in morphology must exist between megaripples and impact ripples. However, when they plotted ripple height against spacing, sorting against spacing, and twentieth-percentile grain size against spacing no discontinuity appeared. Because of this seeming continuity they believed that the same mechanism governed the spacing in both types of ripples, the mechanism being the mean jump distance of saltating grains. Since in the megaripple case small grains bound off larger grains, Ellwood et al. postulated that the jump distance of the smaller grains would increase. By applying a statistical analysis to particle rebound distance they arrived at jump distances of the order of those for impact ripples and megaripples. From this they concluded that characteristic grain path length is responsible for spacing values of all eolian ripples.

Seppala and Linde (1978) investigated ripple development as a function of time and velocity using naturally sorted sediment in a wind tunnel. Each experiment began with a 10 cm bed of sand in the wind tunnel (dimensions 400 cm x 60 cm x 60 cm), and sand flux was erosional. Ripple development was characterized by ripple spacing, and the spacing was measured periodically during each run. This also allowed ripple spacing to be studied as a function of velocity.

Ripple spacing was found to increase with both time and velocity, but the increase was relatively greater with velocity. Ripple plan pattern was observed to become more regular with increasing velocity. An interesting phenomenon

was observed at higher velocities (above 7.5 m/s measured at 10 cm above the bed): ripple spacing initially increased with time, but smaller ripples formed on the stoss slopes of the larger followed by a reduction in spacing (in the larger).

Seppala and Linde also studied sorting in various parts of the ripples. They found that trough material resembled the original bed, crest material was somewhat coarser, but better sorted than the original, and the lee-slope material was poorly sorted. They interpreted the well sorted crestal material as reflecting the uniformity of the saltation process, and the poorly sorted lee-slope as the piecemeal capture of the surface creep.

We can see from the above literature review that our understanding of ripple morphology is incomplete and confused. No consensus exists on what controls the spacing of ripples: Stone and Summers (1972) believe that spacing depends on grain size only, while Bagnold (1954) thinks that spacing depends primarily on wind velocity (and other studies lie somewhere in between). Controls on ripple height are equally uncertain, ranging from sorting (Bangold, 1954) to velocity and grain size (Sharp, 1963). Ripple plan pattern seems to become more regular with increasing velocity, but this is based on only one observation (Seppala and Linde, 1978). Thus, wind ripples are a common bed phase in wind-blown sand, but are poorly understood.

APPROACH IN THIS STUDY

When investigating any fluid-mechanical problem in which the governing equations cannot be solved, a natural approach is to identify important independent variables and to create groups of dimensionless variables from them. This method has been employed in fluvial studies for some time, but has yet to find its way into eolian research. Proposed here is a dimensional analysis for gas-sediment systems.

We must first identify the important system variables. The flow strength must be characterized, and we can use either the mean flow velocity U or the boundary shear stress τ. In addition, the fluid has viscosity μ and density ρ. Important transport properties of the sediment bed are more varied: clearly the mean grain size D and the sediment density ρ_s are vital. Other sediment variables to consider are sorting σ, skewness, shape factors, and a number of other properties probably of minor importance. Lastly, the acceleration of gravity g must be included (Figure 3). So our list of variables is:

> τ or U, ρ, μ, D, ρ_s, σ, g, other sediment properties.

The use of bed shear stress is favored since mean flow velocity is difficult to determine or even define for unbounded gas flows, whereas bed shear stress is easy to determine from the velocity profile. A more convenient form

Figure 3. Important independent variables: μ = viscosity of the fluid; ρ = density of the fluid; τ = bed shear stress; U = mean flow velocity; g = acceleration of gravity; D = mean grain size; ρ_s = density of the sediment; and σ = sorting of the sediment.

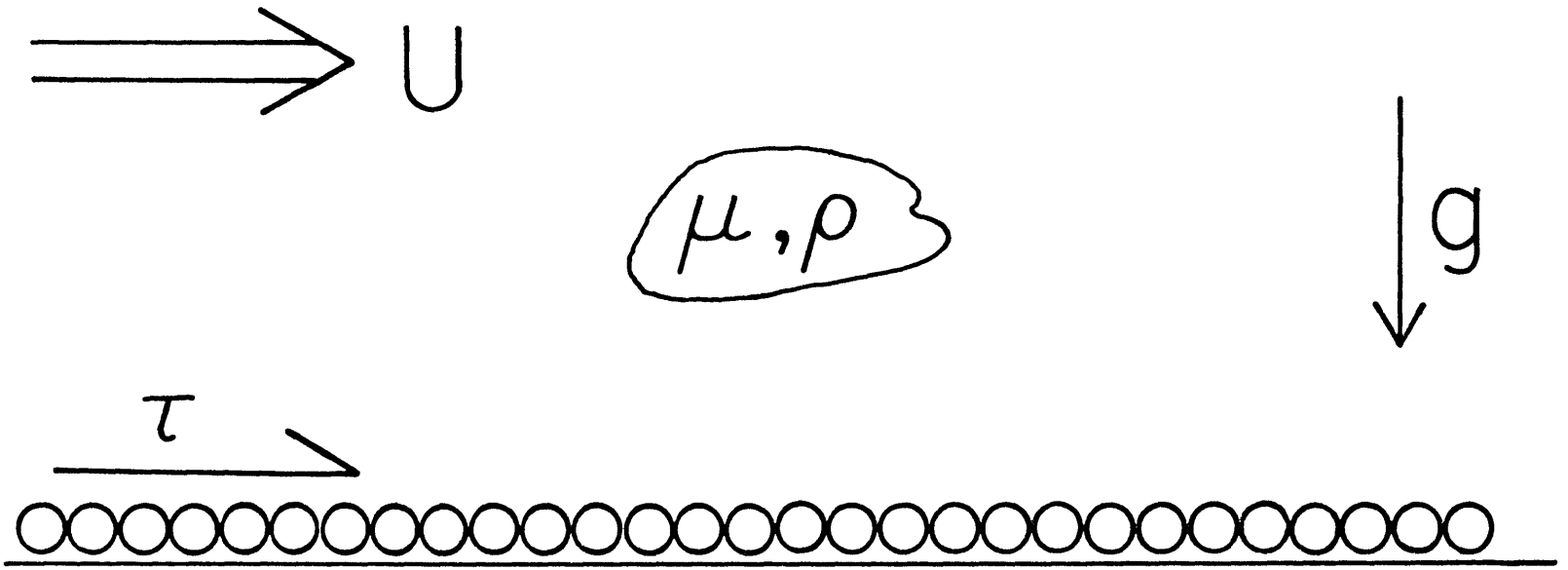

D, ρ_s, σ, other sediment properties

of τ is $U_* = \sqrt{\tau/\rho}$, which is called the shear velocity. So our list of independent variables is now:

$$U_*,\ \rho,\ \mu,\ D,\ \rho_s,\ \sigma,\ g,\ \text{etc.}$$

From this list we form dimensionless variables. By use of the π-theorem (Buckingham, 1914) we may reduce a set of variables by the number of dimensions by forming dimensionless groups. The basic dimensions are time, length, and mass. One set of dimensionless variables is a Reynolds number, a density ratio, a material-properties number, sorting and other sediment variables which are usually already dimensionless:

$$\frac{U_* D \rho}{\mu}\ ,\ \frac{\rho_s}{\rho}\ ,\ \frac{\rho^2 g D^3}{\mu^2}\ ,\ \sigma\ ,\ \text{etc.}$$

In an earthbound system these variables are relatively straightforward: variation in ρ, μ, g, ρ_s, are unimportant. Also, we consider only the effect of D and σ and none of the other size-shape-composition sediment variables. Therefore the final list is:

$$\frac{U_* D \rho}{\mu}\ ,\ \frac{\rho_s}{\rho}\ ,\ \frac{\rho^2 g D^3}{\mu^2}\ ,\ \sigma$$

This list is very powerful and useful: we can change the dimensional variables at will and still describe the same physical situation so long as the dimensionless variables remain constant. In other words, the dimensionless

variables define a mathematical and dynamical space, and we are at the same point in this space regardless of the exact details of the dimensional variables so long as the dimensionless ratios remain the same. This gives us the ability to change the physical scale of the problem (scale modelling), relate data from diverse settings (Mars and Venus for example), or to make experiments with different gases and sediments, and still preserve the dynamics of the problem. As noted above, since we are earthbound μ, ρ, ρ_s, g are essentially constant, so for the purposes of graphical representation we can switch back to the dimensionless variables that are actually nonconstant in this study:

$$U_*,\ D,\ \sigma$$

and be confident that this list is: (1) adequate to completely describe the earthbound problem; and (2) still general in the sense that we can convert back to the dimensionless form for applications to dynamically similar problems provided the list is correct. We will also use the velocity measured at 20 cm above the bed in graphical representations.

In this study certain dependent variables are investigated. These are the ripple height h, stoss slope length i, lee slope length s, overall ripple spacing L (L = i + s), ripple migration rate c, and the center of area o of the ripple profile (Figure 4). These are the same morphologic and kinematic variables investigated by earlier authors,

Figure 4. Important dependent variables: c = ripple speed; o = center of area of the ripple; h = height of the ripple; i = stoss slope length; s = lee slope length; L = ripple spacing.

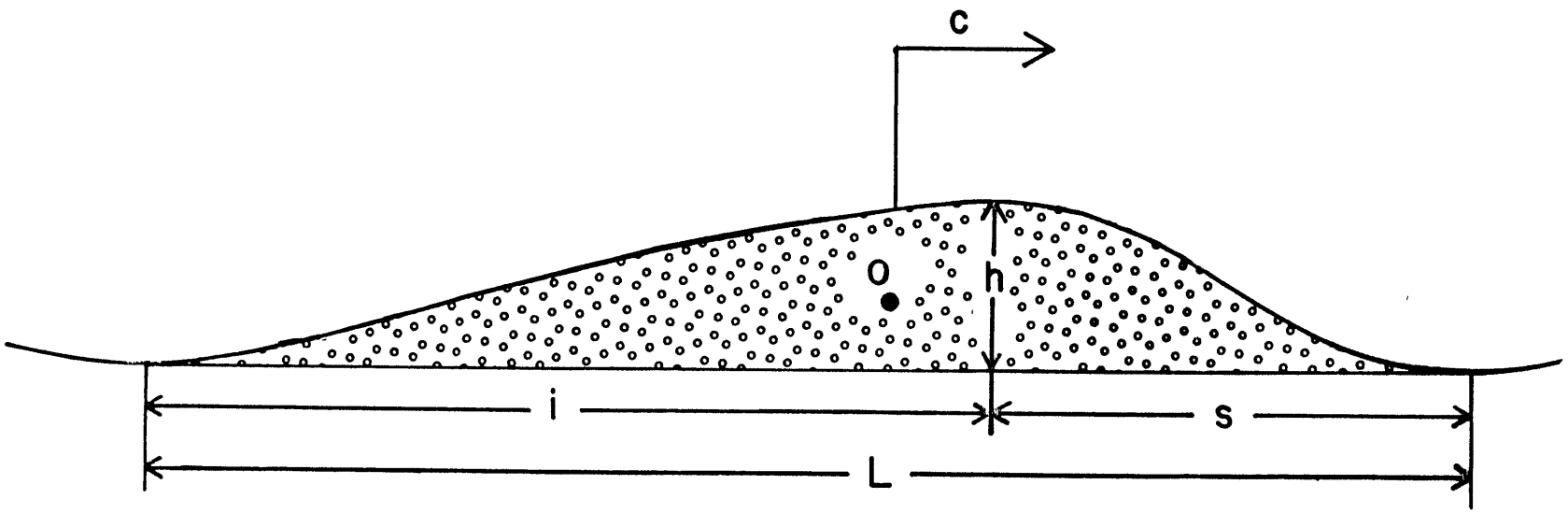
c
O
h
i
s
L

but here are considered dependent variables in a dimensional analysis.

To explore the variation in ripple geometry we systematically varied U_*, D, and σ. The easiest of these to change is U_* by simply changing the flow strength. Much more time and effort are involved in changing grain size and sorting, since sediment must be processed to desired values. The approach in this study is to monitor the responses of morphologic variables to changing U_* for sediment of given size and sorting, then to change the sediment and repeat the process. The variation of U_* values falls between that for initiation of motion, here taken to be the fluid threshold (Bagnold, 1954), and that for flat-bed transport.

Because the grain size and wind velocity have been emphasized in previous studies, we started with a constant value for sorting ($\sigma \simeq 0$) and examined variation of ripple morphology with changing U_* and D. This is something of a repeat of the work of Zingg (1952), as he also used well sorted sands. The reasons for this are fourfold: (1) to observe the processes in well sorted sand firsthand; (2) to better define the curves of velocity versus spacing and height, and to extend Zingg's data to flat-bed conditions; (3) to use more closely spaced grain size intervals; and (4) to clarify differences between Zingg's and Bagnold's data, on the one hand, and the intuitive feelings of the writer on the other.

The mean sizes studied are 0.20 mm (0.18 - 0.22 mm),

0.25 mm (0.22 - 0.28 mm), 0.32 mm (0.28 - 0.36 mm), 0.40 mm (0.36 - 0.44 mm), and 0.78 mm (0.70 - 0.86 mm). When sorting is considered it adds another variable, which greatly complicates and expands the study of ripple morphology. Rather than study a particular sorting for each sand size (other than the well sorted sand) we studied one sorting for one sand size to give further information on the effects of this variable. We used D = 0.44 mm, σ = 0.65 sand in an additional set of runs (Figure 5). This arises from the observation of Ellwood et al. (1975) that spacing can decrease with wind velocity for certain sortings. At lower velocities coarse grains move as creep while at higher velocities they saltate. When the transport mode of these grains changes as a result of increasing wind velocity, ripple spacing decreases, marking the change from megaripples to impact ripples. This change in process is possible only in poorly sorted sands and cannot be present in well sorted sands.

Figure 5. Percent-coarser diagram for '00' sand (D = 0.44 mm) and for vertical sorting experiment.

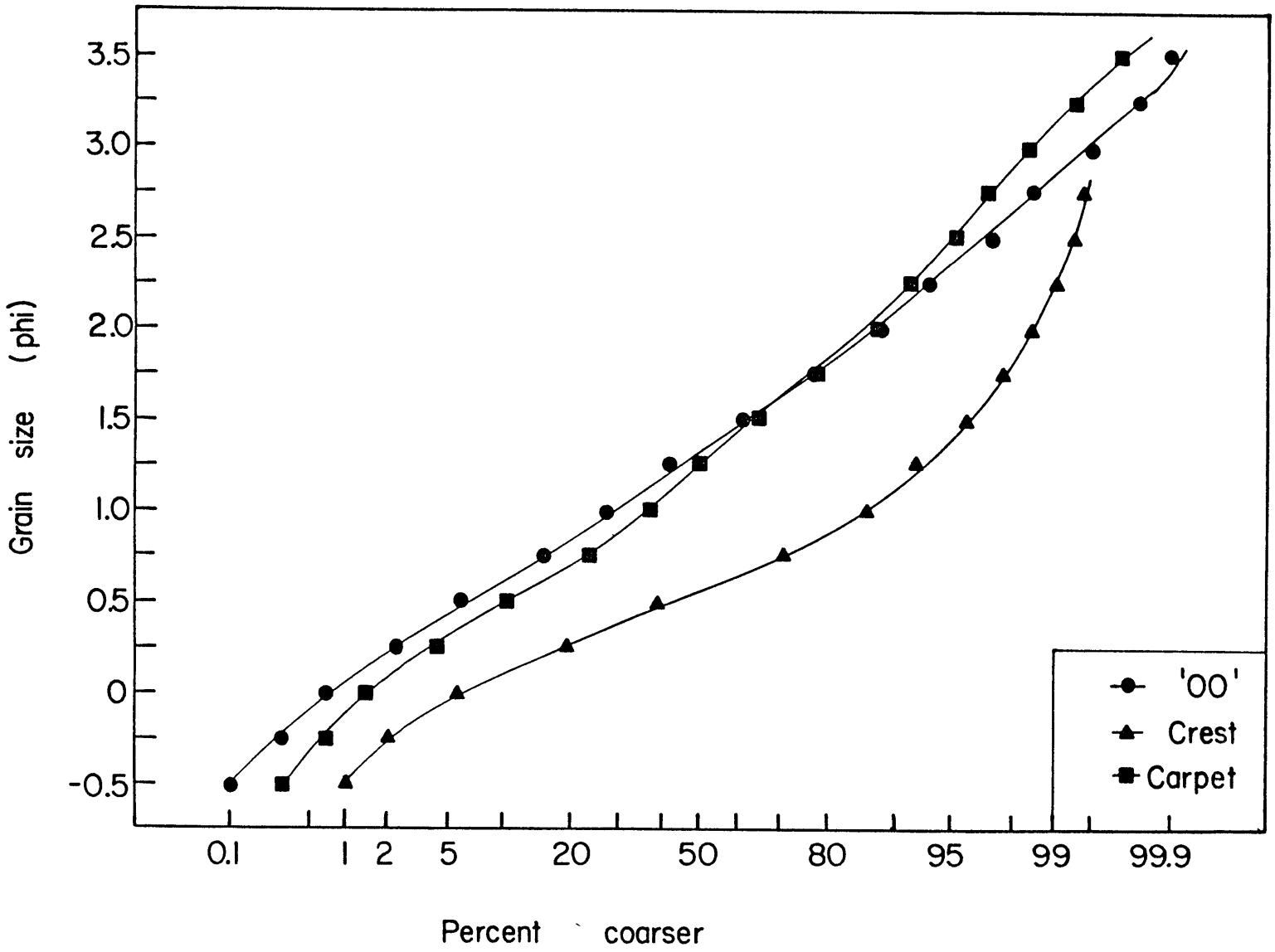
3.5
3.0
2.5
2.0
1.5
1.0
0.5
0
-0.5
Grain size (phi)
0.1
1
2
5
20
50
80
95
99
99.9
Percent coarser
'00'
Crest
Carpet

BASIC FLUID MECHANICS

In the study of eolian ripples, knowledge of certain basic aspects of behavior of turbulent flows is necessary. In addition, properties of sediment-transporting flows must also be considered.

Wall Law

A fluid in steady turbulent flow over a rough surface has a characteristic logarithmic mean-velocity profile given by:

$$\frac{U(z)}{U_*} = C \ln \left(\frac{z}{k}\right) + V \qquad (1)$$

where

$U(z)$ = mean velocity at height z

C = inverse of von Karman's constant

(von Karman's constant = 0.40 for clear flows)

z = height above the sediment bed

k = characteristic roughness height of the surface

V = constant of integration

When sediment is being transported, the relationship becomes:

$$\frac{U(z)}{U_*} = C_1 \ln \left(\frac{z}{K}\right) + V_1 \qquad (2)$$

where

C_1 = inverse of von Karman's constant

Von Karman's constant is taken to be 0.375 (Zingg, 1952) and K and V_1 are determined by projecting measured velocity profiles to small z and noting their "intersection". C_1 must vary somewhat with sediment and wind velocity, but the value taken fits data in sediment-transporting flows, on average, better than the 0.40 value. Zingg found K to be about 10D and V_1 to be about 895D.

Our concern is to find U_*, because it is used to characterize the flow. From the form of Equation (2), we see that if U(z) is known at two different values of z, then U_* is easily determined: U_* multiplied by C_1 is merely the slope of the velocity curve.

Sand-Transporting Flows

When sand-transporting flows are considered, Equation (2) does not hold near the bed. At values of z less than K it is invalid, and near the bed but above z = K a velocity defect is seen in the profile. Bagnold (1954) considers this defect to be negative (velocity measured is actually less than predicted by Equation (2)), while plots of Zingg (1952) seem to indicate a positive defect. Bagnold indicates that this defect is present in the lowermost 2 cm of the velocity profile only.

Owen (1964) produced a detailed analysis of the complete velocity profile in sand-transporting winds. The results are based on two assumptions: (1) the saltation layer acts as a roughness element felt by the flow above; and (2) the

shear stress borne by the fluid at the bed is just sufficient to ensure that the bed is in a mobile state. Owen assumes that the first of these is obviously correct and offers no explanation, and then states that the second is a bit more subtle. Owen proposes that the fluid shear stress at the bed is constant regardless of the wind velocity and that enhanced saltation and creep at higher velocity is the result of the higher energy gained by the bombarding particles while in the flow. The fluid shear stress serves only to create a mobile bed for the saltating grains to strike.

Owen made simple assumptions about the fluid stresses. He took a constant eddy viscosity over the region of the flow affected by saltation by reasoning that the grains entrained in the flow will enhance turbulent mixing. This is unclear because the physics of saltation and the effect of the grains on the flow are poorly understood. Due to the extremely complicated variation of saltation with height and the problem of creating a good energy balance for the flow system, assumptions about the Reynolds stresses are merely guesses until detailed measurements are made in the saltation layer. Presently, the details of viscous stresses, Reynolds stresses, and grain stresses are unresolved.

Bagnold's and Zingg's velocity profiles are somewhat contradictory in regard to a velocity defect: Zingg's is positive and Bagnolds' is negative. This difference may be because Bagnold had only one or two points (on average) outside the saltation layer with which to draw a wall-law

velocity profile, so defects from a log-law are based on equivocal data (Figure 6). Zingg had a minimum of five velocity measurements in the part of the flow unaffected by saltation, so his wall-law extrapolations into the saltation layer should better show the nature of a velocity defect.

Chiu (1972) made much more detailed measurements in the saltation layer than either Bagnold or Zingg, and found a positive defect in velocity near the bed. In fact, his positive defect is observed at heights below 10 cm above the bed, so its presence seems to be well documented.

Saltation and Creep

Much has been made of the mean saltation distance in relationship to ripple morphology, and specifically spacing. Attempts at measuring and computing mean jump distance of saltating grains have been made by Bagnold (1954), Horikawa and Shen (1960), Belly (1964), Kawamura (1951), and Tsuchiya (1970). Each of these studies resulted in a different value for the mean jump distance. Bagnold used a mathematical analysis (unspecified) that assumed that the kinks seen in a semi-log diagram of velocity versus height marked the average height of saltating grains. This approach is fraught with problems: (1) the nature of the velocity profile is poorly understood; (2) the basic assumption that the observed kink in the velocity profile marks the average height of saltating grains is unclear; and

Figure 6. Wind velocity versus height. Profiles of Bagnold (1954) and Zingg (1952). Note the differences in the nature of the velocity defects, and the number of points used by Bagnold to define a log-law line.

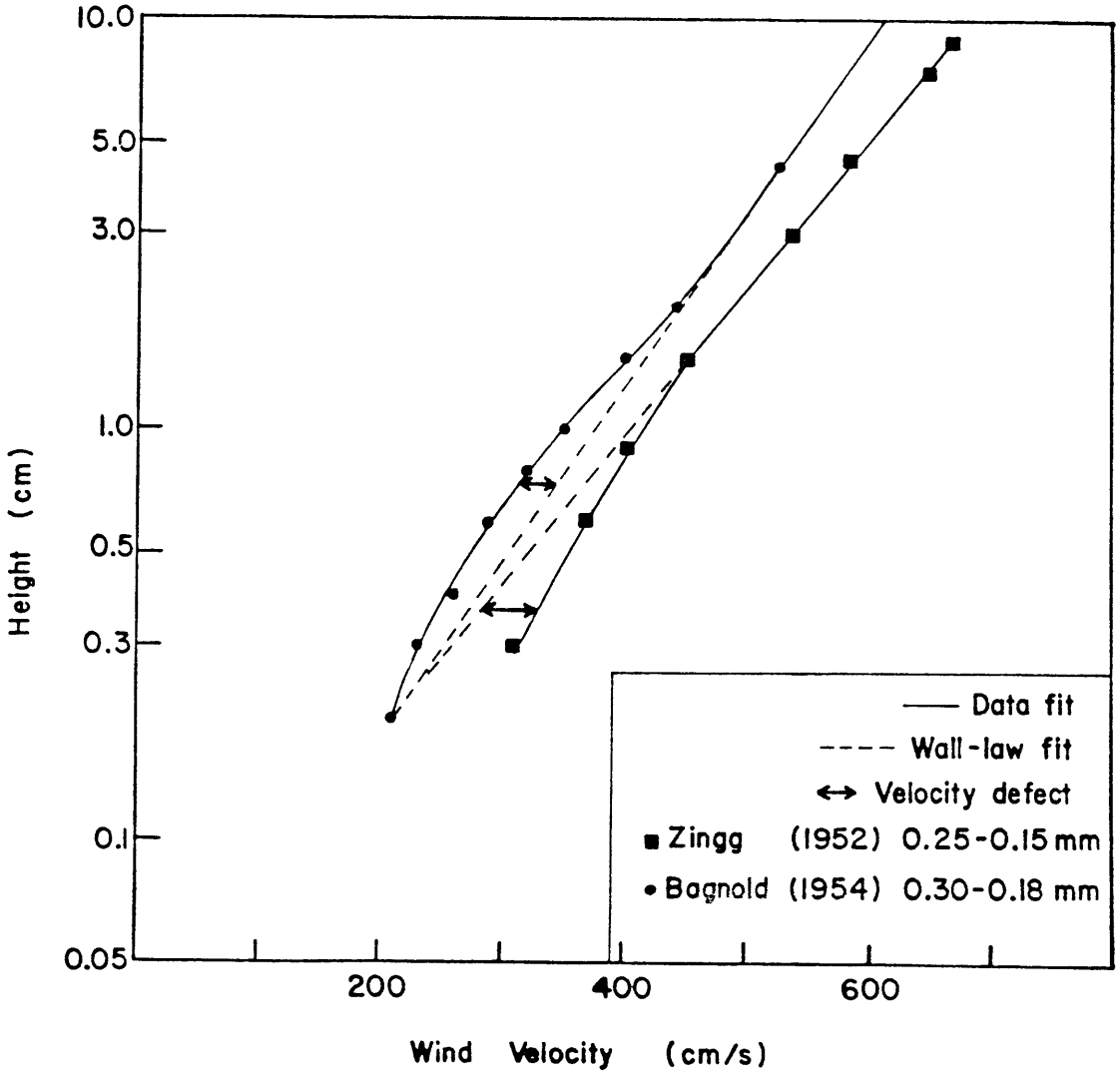
10.0
5.0
3.0
1.0
0.5
0.3
0.1
0.05
Height (cm)
200
400
600
Wind Velocity (cm/s)
Data fit
Wall-law fit
Velocity defect
Zingg (1952) 0.25-0.15 mm
Bagnold (1954) 0.30-0.18 mm

(3) the characteristic path for saltating grains, as defined by Bagnold, does not necessarily give the same velocity profile. Kawamura and Belly used statistical methods to get their values. Horikawa and Shen derived a mean saltation distance by using a horizontal sand trap and finding the mean of the distribution of weight of sand collected with distance. Tsuchiya computed distances for successive saltation of grains using the basic equations of particle motion. Values range from centimeters (Bagnold) to tens of centimeters (Belly).

It is normally assumed that the saltating grains leave the surface vertically. Tsuchiya (1970) found that the take-off angle is typically between 35° and 60° (this was with a few grains in saltation). Most studies to date have examined saltating grains that reach the upper part of the flow and thus probably do have high initial trajectories, but it is possible that grains travelling close to the bed have lower take-off angles. Unfortunately, there has been little study of take-off angles low in the saltation layer, but this must certainly be important since most transport is near the bed.

Surface creep has been little studied. Bagnold (1954) gives the figure that 25% of grains in transport move as creep, a significant fraction. It is commonly assumed that the creep is driven mostly by the impact of saltating grains. Material composing wind ripples moves primarily as creep, so an understanding of the processes involved in creep transport,

i.e., sorting and other mechanical processes, is vital to the elucidation of ripple dynamics. Unfortunately, so little is known about creep movement that few facts can be offered. One speculation concerning vertical sorting of ripple grains was made by Sharp (1963). Noting that ripples have more coarse grains in the crest and travel over a carpet of finer grains, Sharp suggests that this stratification is accomplished by the capture and down-sifting of the finer grains in the interstices of the larger, thus a vertical sorting phenomenon. Bagnold (1954) explains the same observation in terms of differential rates of creep grain movement by the bombardment of the saltating grains: small grains move faster and thus are pushed over the crest, while coarse grains are halted at the crest.

EXPERIMENTAL EQUIPMENT AND METHODS

The main piece of equipment used in the study was a wind tunnel thirty meters long. The tunnel was designed and constructed for studying small-scale eolian bed forms, and required three months to complete. Two additional months were required to fit the tunnel with a pitot-static tube anemometer and to install a flow control system. During the latter period sediment was being processed for tunnel use.

Wind Tunnel

A suction type wind tunnel of special design was built for this project (Figure 7). The requirements on its shape and size were many. The tunnel had to be long enough for full development of the velocity profile and the sediment transport; it had to be as wide as possible to provide the opportunity to study plan pattern of ripples; it had to afford easy access to the working section, to level and to change the sediment; it had to be easy, quick, and cheap to construct; and it had to be easy to instrument. The dimensional requirements were reasonably well met by a tunnel 30 m long, 1.2 m wide, and 0.6 m high, with a 2.4 m cubical collection chamber, which also supported the fan. The tunnel was of suction type for two reasons: to minimize the need for flow straighteners by sucking calm room air through the tunnel and allowing its velocity profile to develop; and to make the walls and tops of the tunnel easier to seal.

The tunnel was constructed from commercial lumber supplies. The base frames, wall frames, and roof frames were

Figure 7. Wind tunnel. Cross section shows the tunnel shape and covers. Covers were held down with framing that extended across the tunnel.

WIND TUNNEL

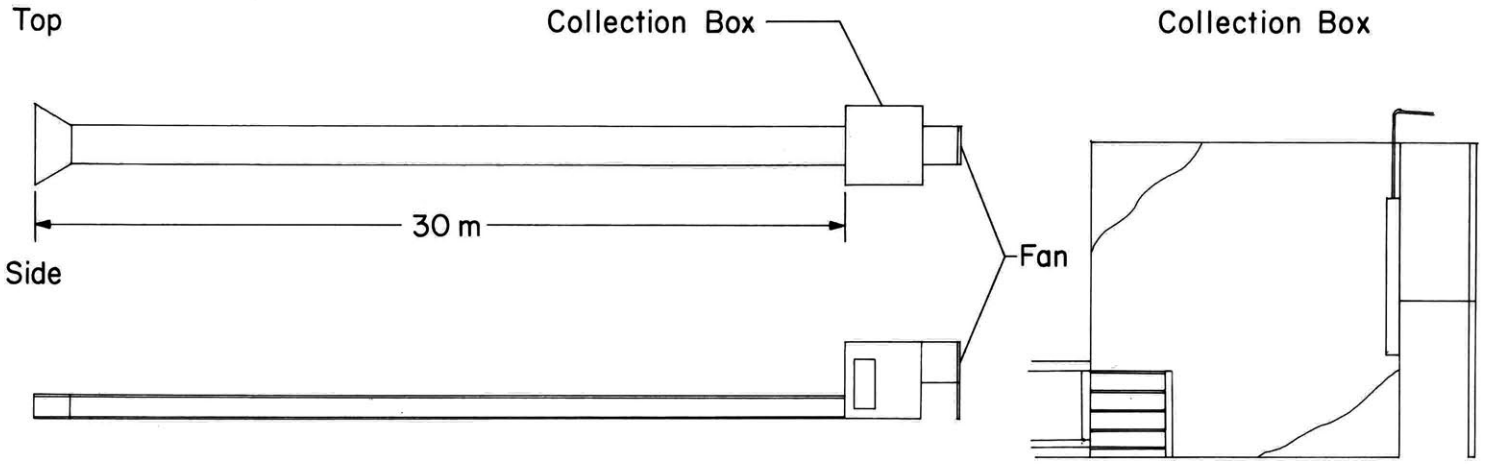
Top
Collection Box
Collection Box
30 m
Side
Fan

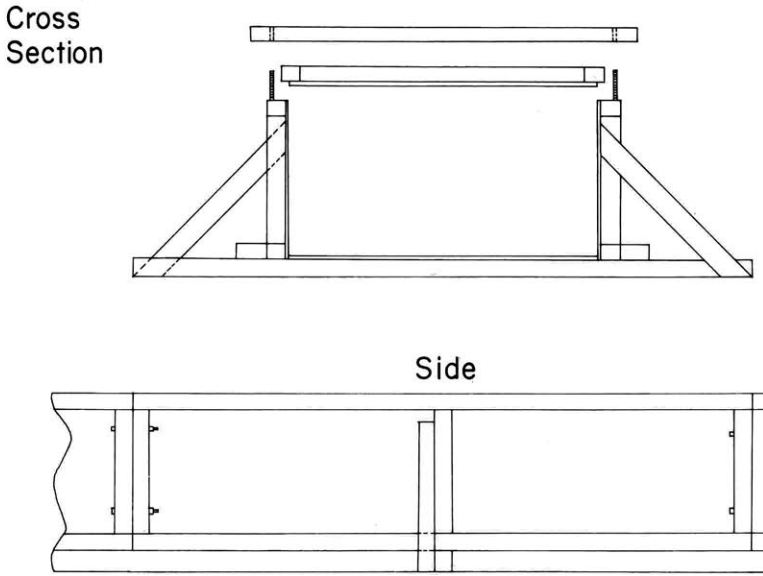
Cross
Section
Side

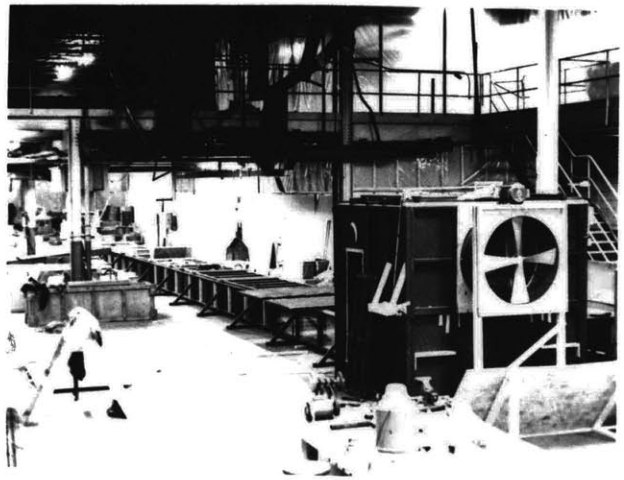

built using standard grade 'A' 2" x 3" framing. The floor sections were built of 4' x 8' sheets of 3/8" particle board and the walls of 4' x 8' sheets (cut in half) of 1/8" masonite. In retrospect, the materials used should have been heavier and stronger in the floor and wall pieces and lighter in the roof sections: the walls and floor were too flexible, and the roof sections were too heavy to be lifted easily by one person. The collection box, which supported the fan assemblage, was constructed of 2" x 3" framing and particle board, with the fan supports consisting of 2" x 4" framing and 4" x 4" posts. The walls of the last 5 m of the tunnel were Plexiglas to provide a test section for observational and photographic purposes.

The fan was a 42" diameter tube-axial type. The tube-axial feature protects the motor from sand remaining entrained in the flow after the collection box. To adjust the flow velocity a movable wall was installed in front of the fan, the amount of wall covering the orifice controlling the flow. The wall was raised and lowered by a rope attached to a hand crank. Also, two 0.6 m x 0.4 m adjustable vents were placed in the collection box to be used for fine adjustments of the flow strength, because the movable wall was held fast to the orifice when the fan was in operation.

Velocity measurements were made using a pitot-static tube connected to an inclined-tube manometer. The bore diameter of the pitot tube was 0.1 mm, and the slope of the manometer (alcohol filled) was 20 to 1. Displacement of the

manometer level could be read to 1 mm (± 1 mm) for an accuracy of better than 0.05 m/s in velocity. Since the tube bore was so small, response time was on the order of 60 seconds, so the velocity measured was a mean velocity. Because the displacement varies as the square root of velocity, accuracy increased at higher velocities. The pitot-static tube was mounted to a 2.5 cm x 10 cm x 100 cm rounded staff that was raised and lowered into the tunnel. A slot was cut in the tunnel roof to give the tube assemblage streamwise mobility along the tunnel.

Actual measurements of the ripples required several pieces of equipment. The ripple spacing was measured using a meter stick and low-angle lighting. Ripple height was measured using a point gauge mounted on a movable carriage. The carriage moved on a removable track mounted on the tunnel wall. Owing to the tunnel size and the fact that measurements were made at the tunnel centerline, observation of the point contacting the bed was extremely difficult and inaccurate. To alleviate this problem the end of the point gauge was viewed through a three-power telescope. The telescope viewed the reflection of the point gauge in a mirror, allowing low-angle observations to be made from above. Bed height could be measured with a repeatablility of ± 0.02 mm, the point gauge reading to 0.01 mm.

Tunnel Flow Characteristics

The flow in the wind tunnel is fully developed turbulent

duct flow at a distance of 5 m from the entrance. Unfortunately, after initial runs were completed, it became obvious that the flow had three-dimensional aspects. Most of the three-dimensionality was related to the entrance geometry, and the lack of flow straighteners. When flow straighteners were installed (60 cm lengths of paper-towel tube just upstream of the entrance), the flow was acceptably two-dimensional near the centerline of the tunnel. However, it was then discovered that secondary circulations were present due to the small 2:1 width/height ratio of the tunnel. Four sets of circulation were present in the tunnel. Work of Hussain and Reynolds (1975) and the advice of Professor M. Crawford (MIT Department of Mechanical Engineering, personal communication, 1979) indicate that at least a 3:1 width/height ratio is needed to reduce these circulations to an acceptable level. While in our case the presence of secondary circulations is not a serious problem (see discussion below), this information raises serious questions about previous studies in which tunnel cross-sections are typically 1:1.

To help reduce these circulations further, two horizontal plates 2 m long were installed in the tunnel 15 cm above the bed and below the roof at a point upwind of the sand bed (this was done on the advice of Professor Crawford). This alleviated most of the effects of the circulations (lateral movement of sand and three-dimensionality of the flow) upwind and over most of the length of the sand bed.

Fortunately, the centerline of the tunnel, where all the measurements were made, was a null point in the circulation pattern. This is the same approach used by Seppala and Linde (1978), who also reported secondary circulations. Since the centerline is a null point, it receives little added saltation or creep input, so the processes are fairly two-dimensional. Another potential problem in the flow structure of this tunnel is the interference of wall and top boundary layers, but since this is uncontrollable, it was accepted and not evaluated.

Because of the desire to make equilibrium runs (steady sand flux), a sediment-feed device was installed. This consisted of a funnel-shaped hopper mounted on the roof of the tunnel at the upwind end of the sand bed to feed sediment into the flow from above. The need for a sediment feed to hasten the development of the transport profile was demonstrated by Bagnold (1954) and Belly (1964). This writer made three sets of runs to check the development of the transport profile. During the first set sand was fed from the roof, and development of transport was monitored by sand traps spaced every 3 m down the length of the tunnel. The sand feed led to essentially uniform transport. When this was repeated at the same velocity but without the sand feed, a monotonic increase in the quantity of sand collected in each trap was found down the length of the tunnel, demonstrating the incomplete development of the tranpsport profile. To test whether the system could be overfed, a third set

was made at a higher velocity with the sand feed opened all the way, introducing much more sand than could be normally transported by the flow. In this case the first sand trap had more sand than the others, and a mound of sand was deposited under the sand feed, but each trap downwind showed essentially equal rates of transport. This was significant to demonstrate, because the transport profile can be brought quickly up to equilibrium by the introduction of sediment into the flow, but it is difficult, if not impossible, to induce greater-than-equilibrium transport regardless of the feed rate.

Sediment Preparation

Special sand was needed for the runs with well sorted sediment, but owing to the difficulty of purchasing large quantitites of essentially unisize sand and the tedium of using standard small sieves, other processing equipment was built. The first large-quantity sieve used was a motor-driven 8' x 3' rectangular tilting screen. This was less than satisfactory because it required constant operator attention, and it was difficult to clean. The next sieve used was a barrel type with automatic feed and removal, and provided continuous operation with little attention. A raised reservoir barrel fed sand into a rotating screen drum with a horizontal axis with the fine fraction falling through the screen and the coarse fraction passing through the drum for collection. The sieving capacity was about

one cubic foot per hour. In addition, the sieve was arranged to be self-cleaning by mounting a stiff-bristle broom to rest against it. The sediment used in the runs with well sorted sand was glacial outwash sediment that was dominantly quartz. Sand for the runs with poorly sorted sediment was type '00' blasting sand purchased from the Holliston Sand Company, Holliston, Massachusetts. It has a mean size of 0.44 mm and a sorting of 0.65 (phi units).

For size analysis, standard 8" U.S. standard half-height sieves at 1/4 phi intervals were used in a Ro-tap sieve shaking machine.

Photography

Photographs were taken of all the runs. To aid in comparison of runs, identical camera positions were used. Lighting is important, so three reflecting spot-lamps with 150 watt bulbs were placed perpendicular to the ripple trend at a low angle to the surface to enhance ripple geometry. A 35 mm camera with a 50 mm lens was used to take the pictures. Also, a time-lapse movie was shot using the same lighting arrangement.

Sand Traps

For qualitative study of the development of transport profiles, a set of sand traps was constructed. These consisted of Plexiglas tubes 30 cm long and 3 cm in diameter mounted on steel rods. These were set level with the sediment surface and oriented parallel to the flow. While these

traps are certainly inefficient and inaccurate, they provide good qualitative estimates of the relative amount of sand in transport at different stations in the tunnel.

Procedure for Runs

The same procedure was followed in every run:

1) The bed was levelled using a scraper whose bottom edge was parallel to the tunnel floor.

2) Sediment in the collection box was removed and put into the feed hopper. In runs with poorly sorted sediment, the sand in the collection box was mixed into the sand in the tunnel before levelling to ensure that no downwind sorting was created so that sediment sorting remained an independent variable.

3) Covers and instruments were put back into place. Fan opening was adjusted for the next run.

4) The tunnel was turned on, the sediment feed started, velocity profiles recorded, and pictures taken. Qualitative observations on ripples and transport were made.

5) The fan was turned off and more photographs taken.

6) The covers were removed and ripple geometry measured. Ripple measurements consisted of measurements of spacing and height over all ripples in the test section and of a profile over four ripples with height measured every 0.5 cm or 1.0 cm. Ripples were not measured if three-dimensional aspects were present, i.e., bifurcation at the

measurement point.

Only about half of the tunnel length was used during the runs with well sorted sand. Because of the limited quanitity of sediment (since sediment processing required so much time), a 2 cm bed was spread across the tunnel floor over half of its length. This provided more than ample depth for ripples, and no scour was present in the test section. There was erosion at the point of the sand feed because of the high energy of grains falling from the tunnel roof, but sediment scoured was deposited well upwind of the test section: a minimum of 3 m of equilibrium sand transport was present in the region upwind of the test section. The steadiness of transport was determined by the constancy of ripple spacing and the zero net accretion of the bed downwind of the initial deposition due to the scour. In the runs with poorly sorted sediment all but 4 m of the tunnel length was used.

Determination of Run Time

Each experiment lasted long enough to ensure full development of the ripples. This was tested by allowing several runs to continue for up to an hour with ripples measured every 5 or 10 minutes. This was done for each sand size to get a qualitative idea of development time. An average time for full development (ripple geometry constant) was 12 minutes. Every run lasted at least 20 minutes to ensure that ripples were in equilibrium with the flow.

Plan pattern also gave insights into the stage of ripple development. At first, at the start of a run, ripples are quite three-dimensional, with bifurcations and cross-connections (that aid in ripple growth). At equilibrium the ripples are two-dimensional in the center of the tunnel, with bifurcations remaining common near the walls only. Each run continued until the latter condition was achieved.

Measurement of Ripple Morphology

Features of ripple morphology measured were spacing, height, and profile (to determine asymmetry). Ripple spacing was determined by measuring a set of ripples, beginning and ending in a trough, and dividing the distance by the number of ripples. Between twenty and forty ripples were measured for each run, with a measurement repeatability of $\pm$ 2mm for a set. Heights were measured using a point gauge for the same ripples used in the spacing determinations. To determine asymmetry index A and general ripple shape, four ripples were profiled by measuring heights every 1 cm or 0.5 cm. These data were smoothed to eliminate measurement error using a truncated Fourier series. A computer program was written to take the data and compute a Fourier sine series. The series was truncated at about one-half or one-third of the number of data points in order to fit a smooth curve through the points. Asymmetry index was measured by integration of the sine series to find the center of area of the ripple profile (for each ripple),

starting at the upwind trough, and then dividing by the ripple spacing. If A = 0.5, the ripple is symmetrical (center of area halfway between troughs), if A>0.5, the ripple is asymmetrical downwind, and if A<0.5, the ripple is asymmetrical upwind. Bed forms such as dunes are asymmetrical upwind, see Figure 8 for other examples. All data on ripple morphology were collected in the last 3.5 m of the tunnel.

Figure 8. Examples of asymmetry index. Dot in ripple marks the center of area (horizontal). Note that the asymmetry index is sensitive to changes in ripple shape.

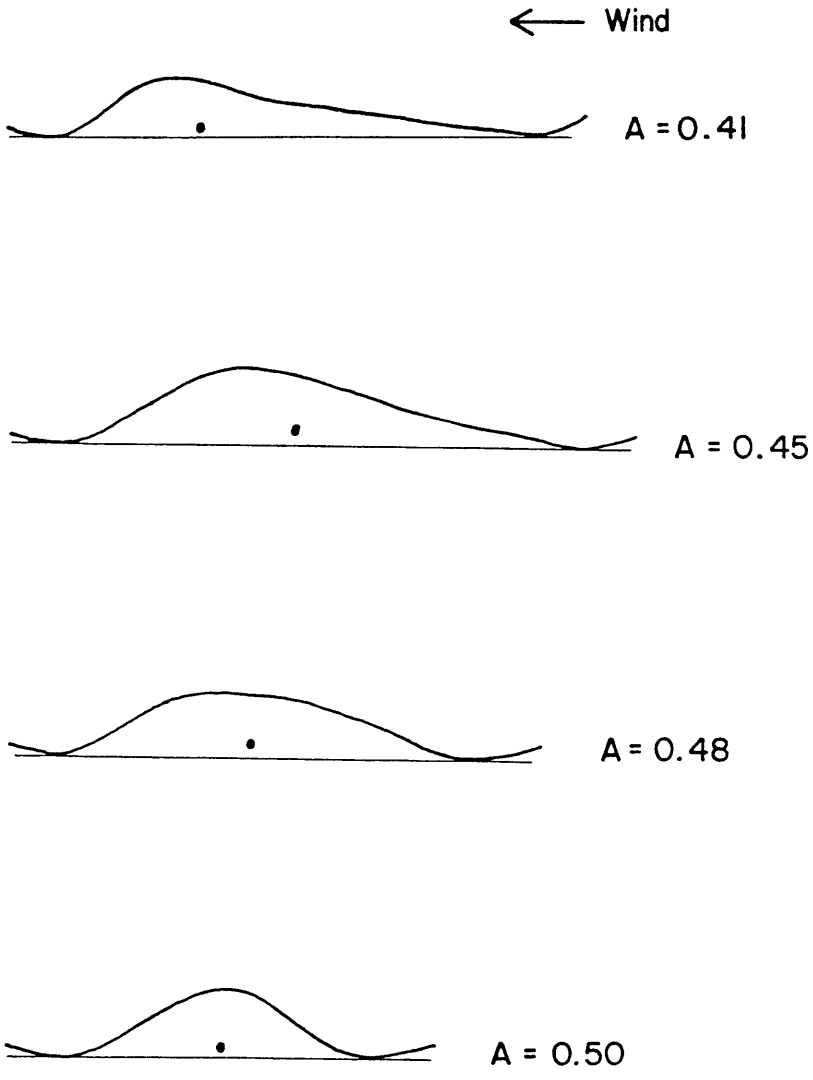

Examples of ripple asymmetry index

RESULTS

The following section summarizes the results of the runs and deals with the behavior of each sand and the nature of the velocity profiles. The majority of runs involved well sorted sand, and for each sand, values of U_{20} (the velocity at 20 cm above the bed), U_*, L, h, and A are presented. Results will be described in both written and graphical form, and base data are given in Appendix 1.

Sand 0.78 mm

This was the coarsest sand used in the study. Ripple spacing increased with increasing velocity and height first increased and then decreased (Figure 9). These trends result in ripple index first decreasing and then increasing. No clear trend in A is present, and ripples appear symmetrical.

Ripples develop from a flat bed in the same manner observed by Cornish (1914) and Sharp (1963): the first bed configuration that develops consists of small mounds of sand, which give the surface a mottled appearance (Figure 10). These form in the first two or three minutes of a run. By ten minutes into the run recognizable ripples started to form from these mounds (Figure 11), and by fifteen minutes well formed ripples extending across the tunnel developed (Figures 12, 13) that are in equilibrium with the flow (constant L and h). An important feature of the tunnel is that the wind ceases the instant the fan is turned off so that a waning-flow modification is totally absent.

Figure 9. Morphology data for 0.78 mm sand. Error bars on spacing and height correspond to one standard deviation unit. Bars on plots involving shear velocity correspond to maximum error of all points. A. Ripple spacing and height versus velocity at 20 cm above the bed. B. Ripple index versus U_{20}. C. Asymmetry index versus U_{20}. D. Ripple height and spacing versus shear velocity. E. Ripple index versus U_*. F. Asymmetry index versus U_*

A.

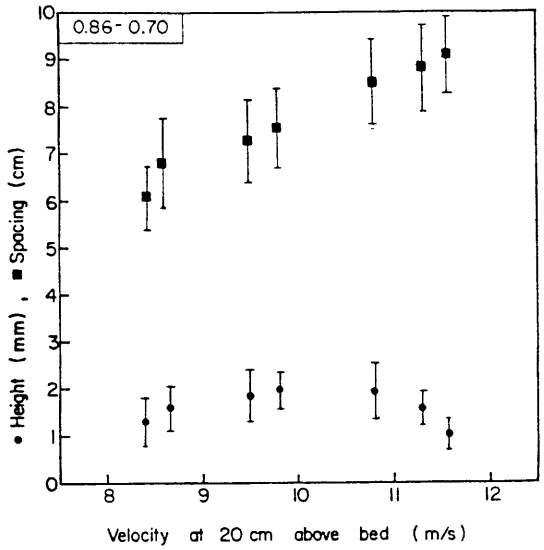
0.86-0.70
• Height (mm), ■ Spacing (cm)
Velocity at 20 cm above bed (m/s)

B.

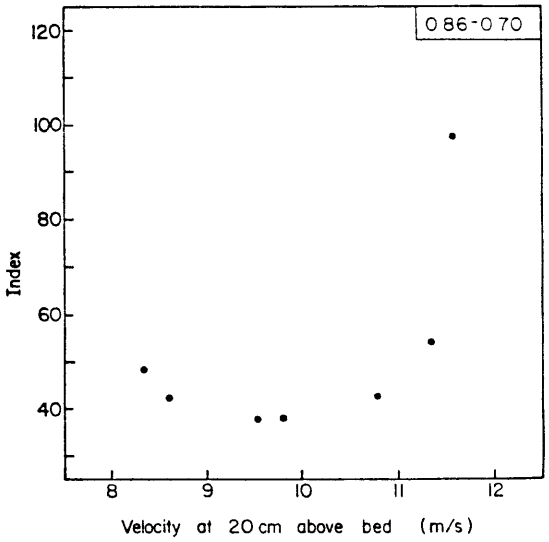
0.86-0.70
Index
Velocity at 20 cm above bed (m/s)

C.

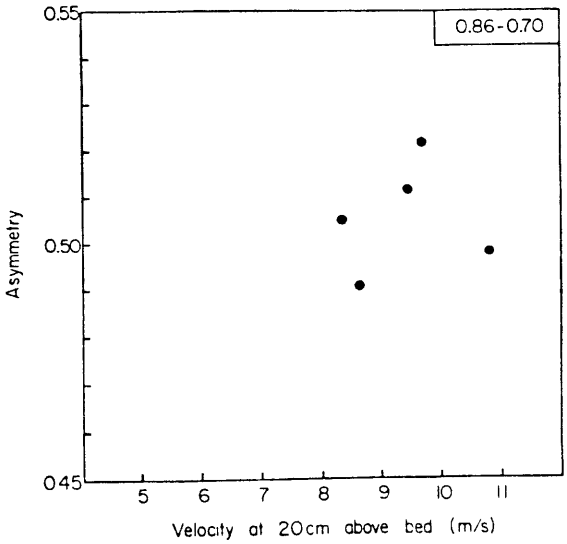
0.86-0.70
Asymmetry
Velocity at 20cm above bed (m/s)

D.

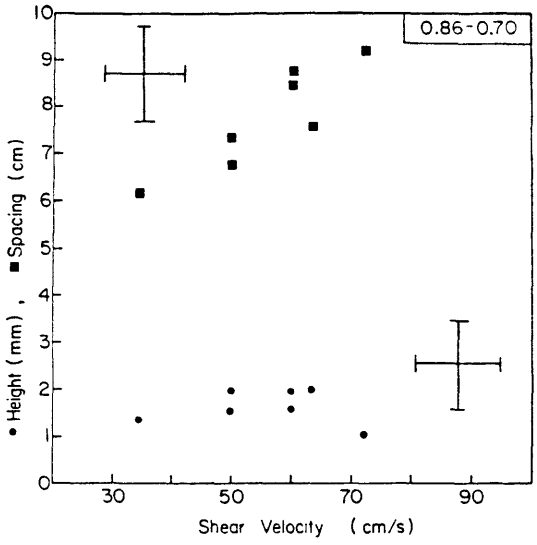
0.86-0.70
• Height (mm) , ■ Spacing (cm)
Shear Velocity (cm/s)

E.

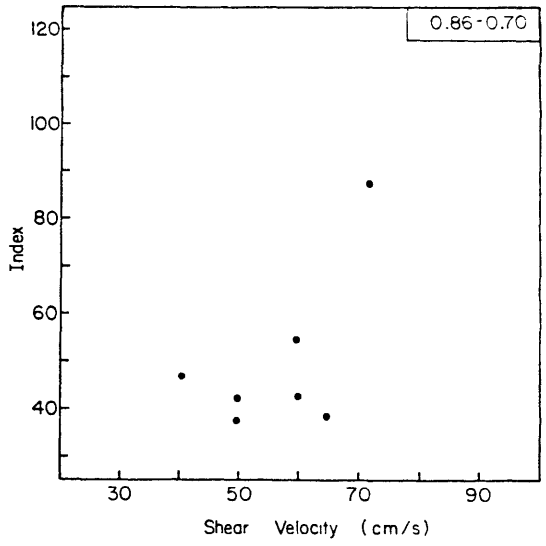
0.86-0.70
Index
Shear Velocity (cm/s)

F.

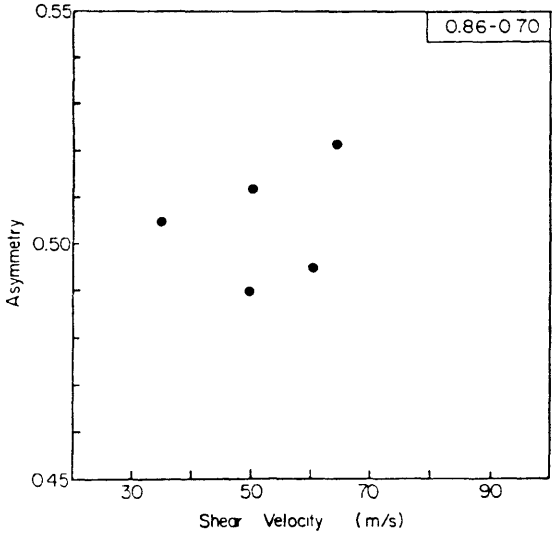
0.86-0.70
Asymmetry
Shear Velocity (m/s)

Figure 10. Photograph five minutes after start of run in 0.78 mm sand.

Figure 11. Photograph ten minutes after start of run in 0.78 mm sand.

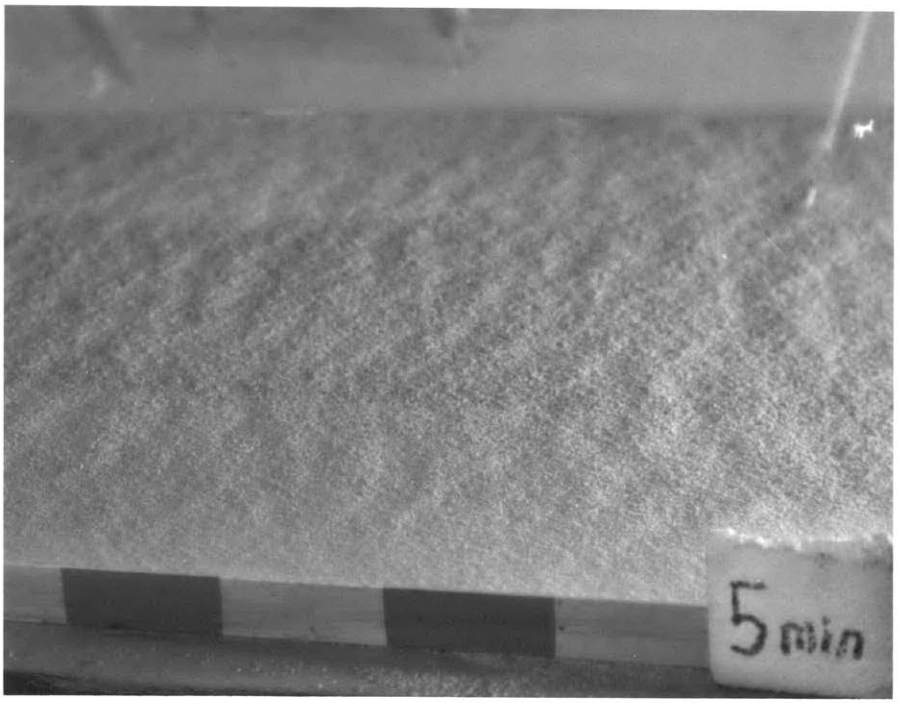
5 min

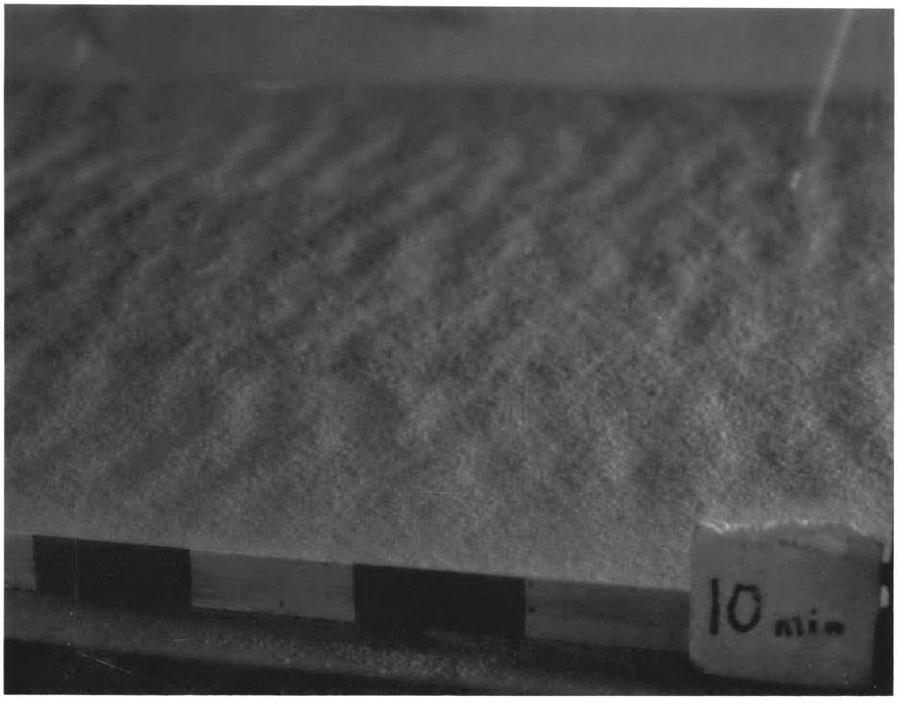
10 min

Figure 12. Photograph fifteen minutes after start of run in 0.78 mm sand.

Figure 13. Photograph twenty minutes after start of run in 0.78 mm sand, end of the run.

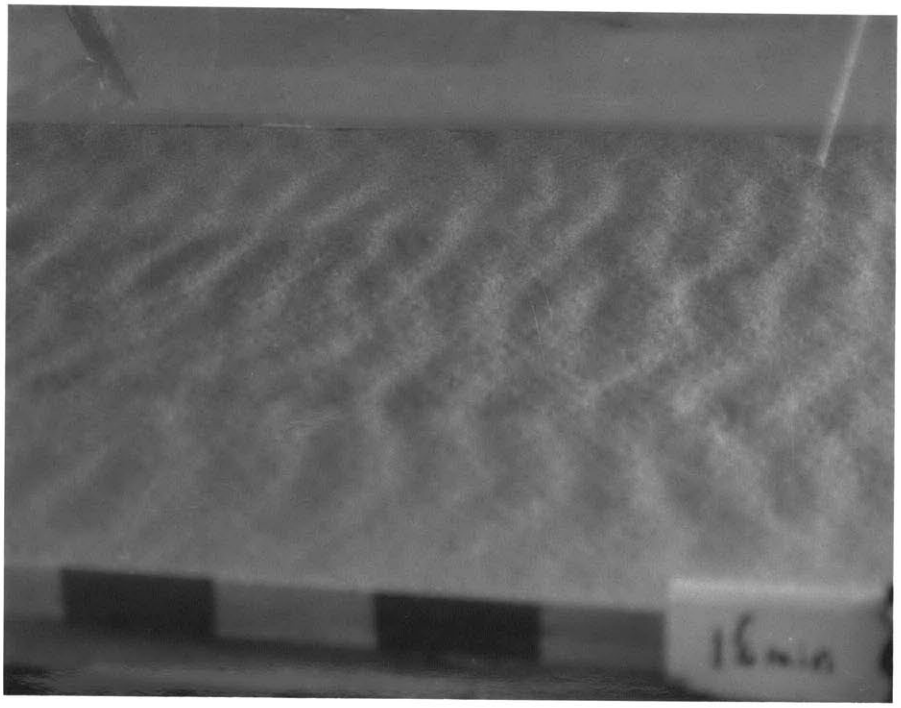
16min

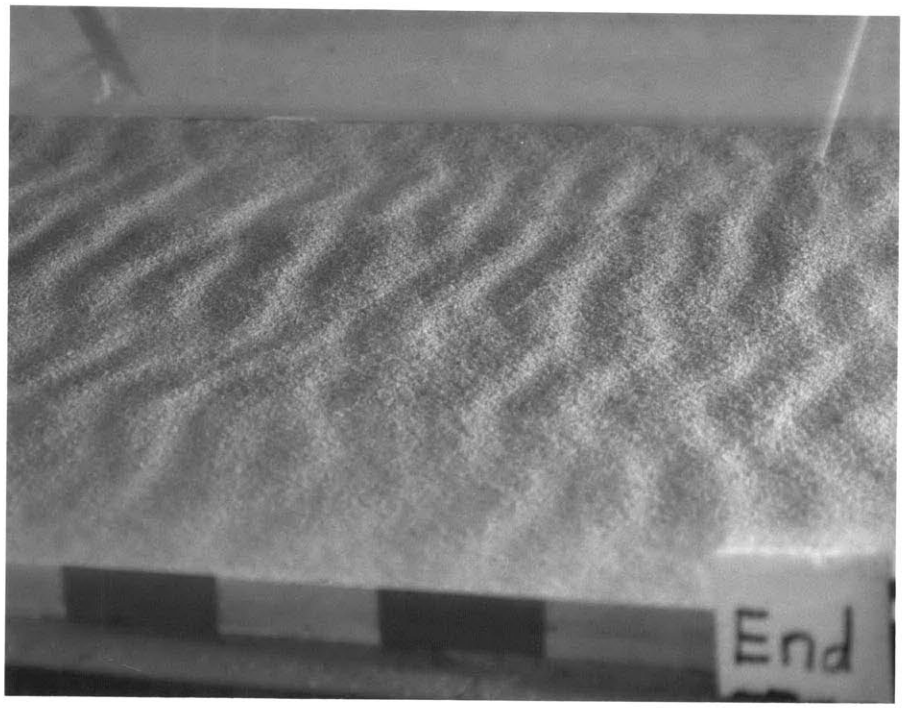
End

Sand 0.44 mm

This sand and the others smaller were chosen to (1) better define the transition in behavior from coarse to fine sand noted by Zingg (1952); and (2) collect detailed data on grain sizes most common in eolian deposits. Ripple spacing in this sand increased with increasing flow strength, and in a way similar to that observed by Zingg (1952): the increase is gradual at first, but then more rapid at higher velocities (Figure 14). Again, as observed by Zingg, the point of inflection is manifested in the ripples as a point where spacing, height, and plan pattern of the ripples become quite irregular (Figure 14, 15). While this change is not strikingly demonstrated in plots of spacing, it is quite apparent in plots of ripple index versus U_{20} and U_* as a sudden increase in I at about U_{20} = 9.5 m/s, U_* = 60 cm/s (Figure 14). Ripple development over all flow strengths was similar to that described by Cornish (1914).

Sand 0.32 mm

Ripple spacing increases and height decreases with increasing velocity, as seen in Figure 16. Again, ripple index increases with velocity, though rather slowly at lower velocities, and asymmetry index is scattered about A = 0.5. Development is the same as described above, but the time required to reach equilibrium is quite short, of the order of 7 minutes at most. Important to note is that spacing increases smoothly with velocity and does not show the

Figure 14. Morphology data for 0.40 mm sand. Error bars and plot labels the same as in Figure 9.

A.

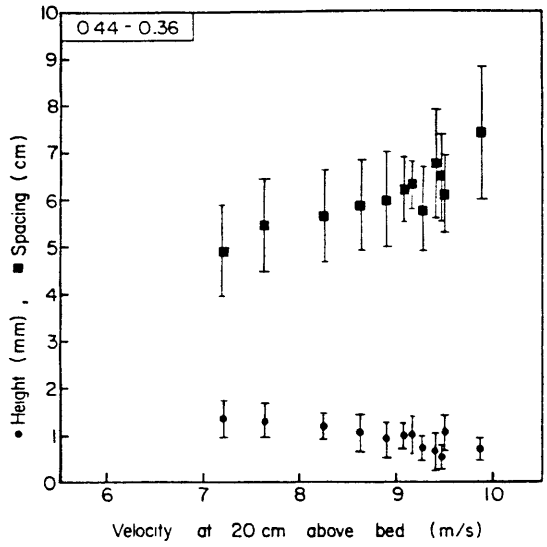
0.44 - 0.36
• Height (mm) , ■ Spacing (cm)
Velocity at 20 cm above bed (m/s)

B.

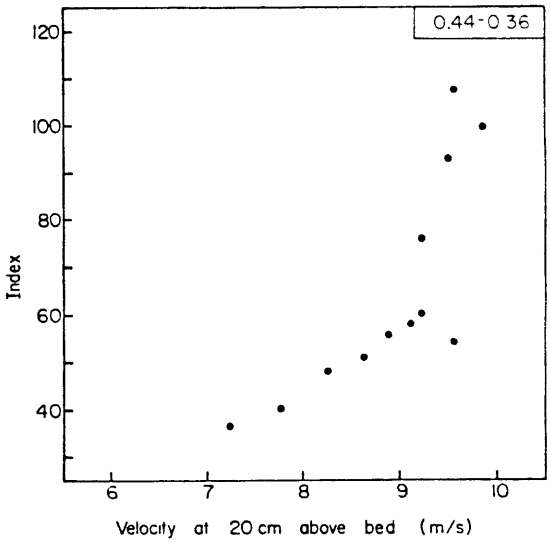
0.44-0.36
Index
Velocity at 20 cm above bed (m/s)

C.

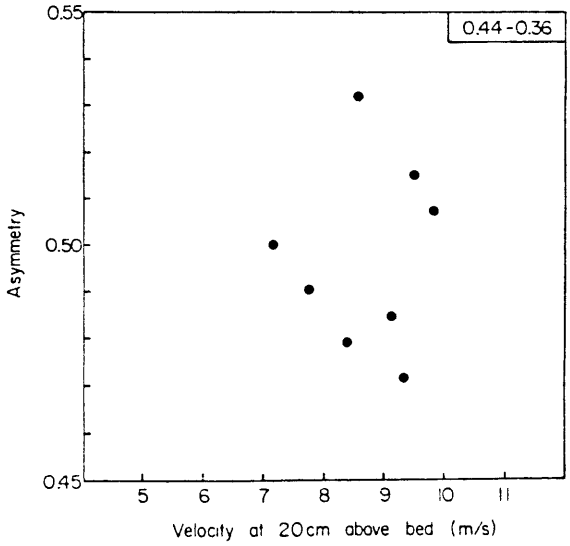
0.44-0.36
Asymmetry
Velocity at 20cm above bed (m/s)

D.

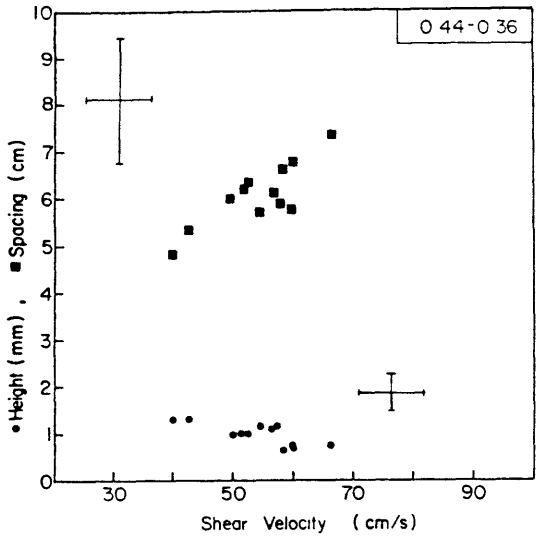
0 44-0 36
• Height (mm) , ■ Spacing (cm)
Shear Velocity (cm/s)

E.

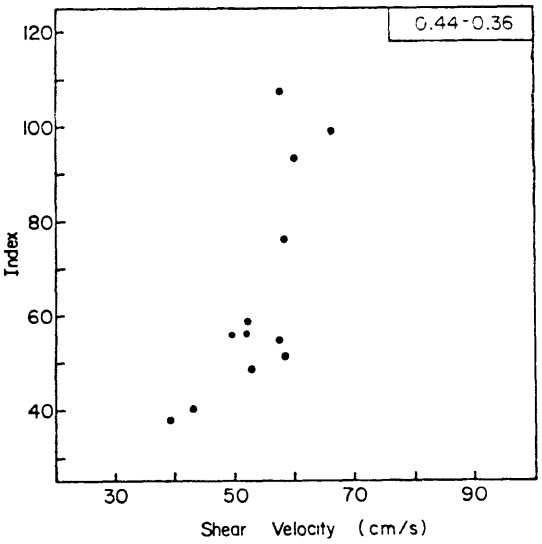
0.44-0.36
Index
Shear Velocity (cm/s)

F.

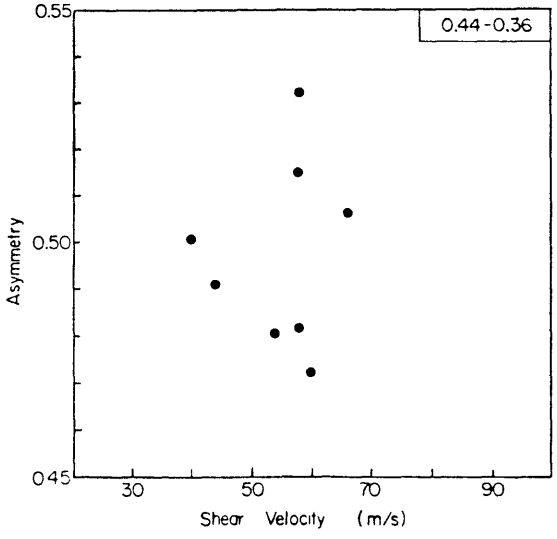
0.44-0.36
Asymmetry
Shear Velocity (m/s)

Figure 15. Photograph of ripples around the change in spacing behavior in 0.40 mm sand. Ripples are regular at sides of tunnel, but irregular in the middle due to the boundary layers of the walls.

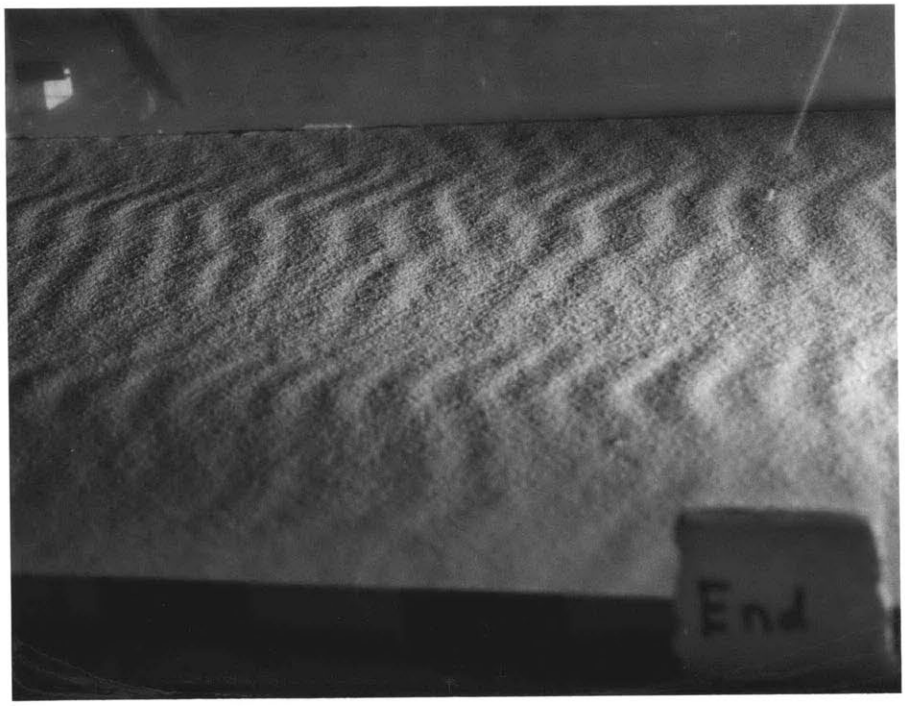
End

Figure 16. Morphology data for 0.32 mm sand. Error bars and labels the same as in Figure 9.

A.

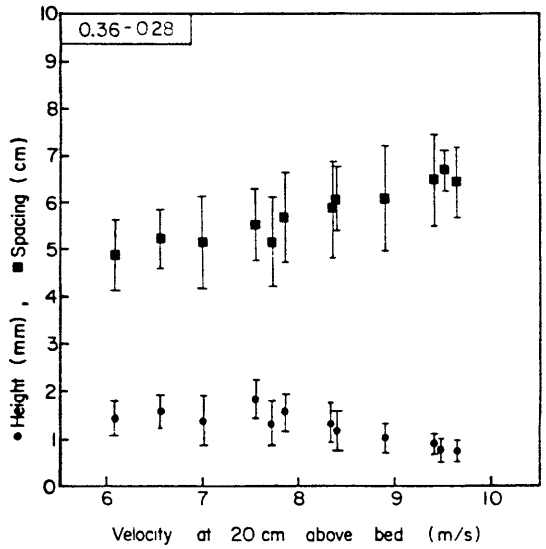
0.36-028
• Height (mm) , ■ Spacing (cm)
Velocity at 20 cm above bed (m/s)

B.

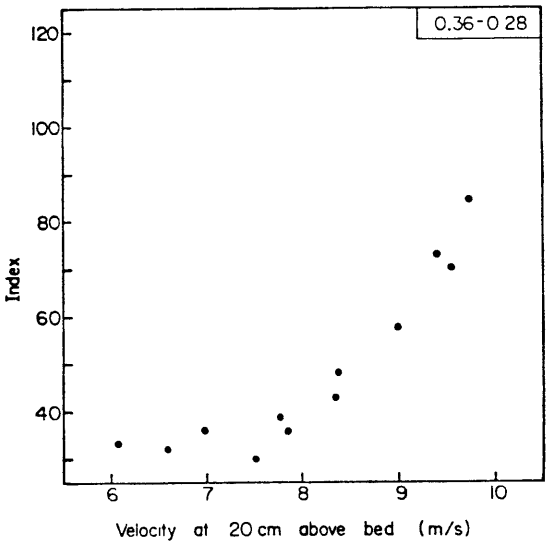
0.36-0 28
Index
Velocity at 20 cm above bed (m/s)

C.

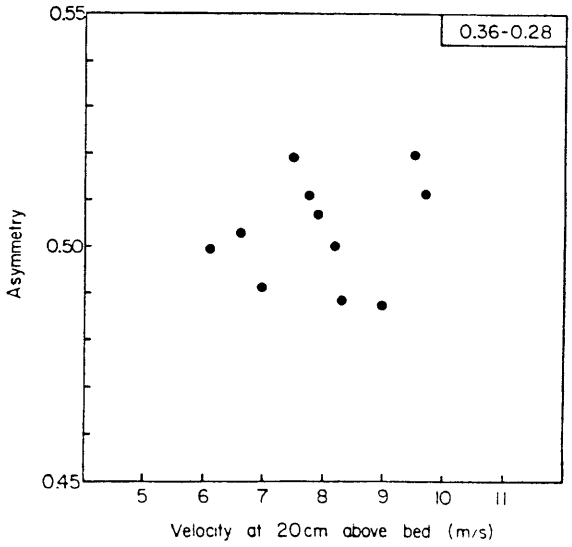
0.36-0.28
Asymmetry
Velocity at 20cm above bed (m/s)

D.

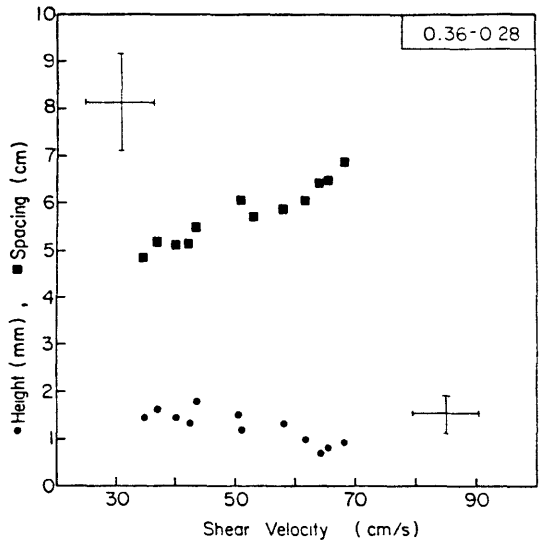
0.36-0.28
•Height (mm) , ■Spacing (cm)
Shear Velocity (cm/s)

E.

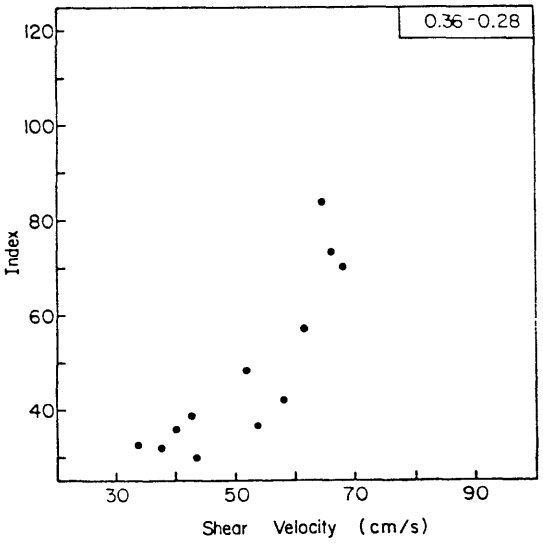
0.36-0.28
Index
Shear Velocity (cm/s)

F.

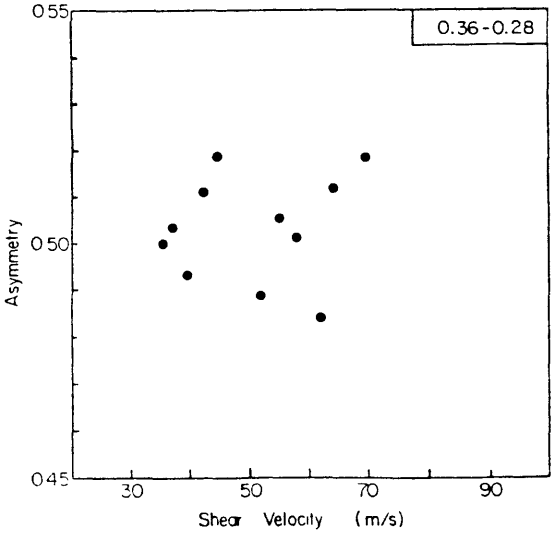
0.36-0.28
Asymmetry
Shear Velocity (m/s)

inflection of the previous sand.

Sand 0.25 mm

Ripple spacing increases, height decreases, and ripple index on average increases with increasing velocity (Figure 17). The nature of the increase of spacing with velocity is interesting: a flat spot of constant spacing with increasing velocity and then a rapid increase in spacing with velocity are present at higher velocities. No clear trend in asymmetry index is present. Ripple development at velocities below U_{20} = 9.0 m/s is similar to that outlined by Cornish, but above this value ripples are the first bed configuration to form (the mottle stage is completely absent), though the ripples that form have lower-than-equilibirum spacing. This change in mode of ripple development corresponds to the area of essentially constant spacing with increasing velocity in the plot of U_{20} versus spacing.

Sand 0.20 mm

This sand, the finest used, had a radically different behavior of morphology as a function of velocity. Spacing increases rapidly with increasing velocity (the largest ripples produced in the study were in this sand), and the change of height with velocity is quite irregular (Figure 18). Ripple development followed the scheme mottles-to-ripples at the lowest velocity, but at higher velocities was characterized by ripples being the first bed configuration to form from the flat bed. Ripples also require a longer

Figure 17. Morphology data for 0.25 mm sand. Error bars and plot labels the same as in Figure 9.

A.

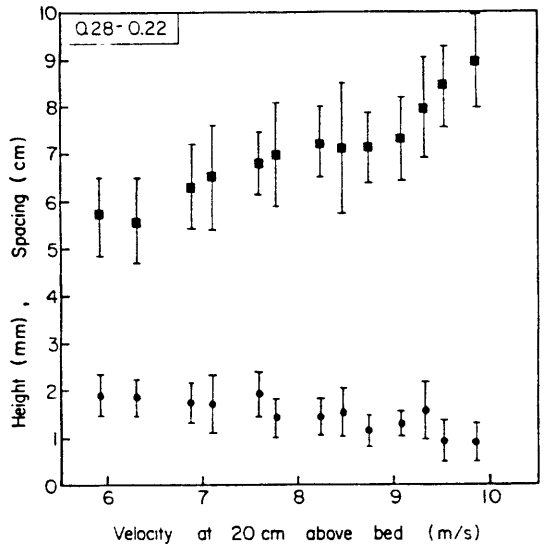
0.28-0.22
Height (mm), Spacing (cm)
Velocity at 20 cm above bed (m/s)

B.

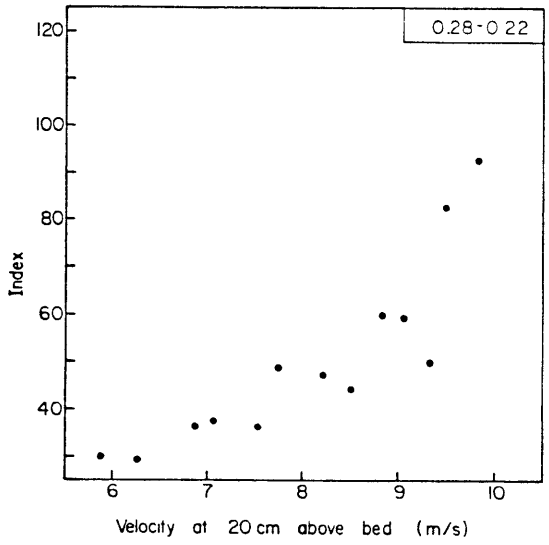
0.28-0.22
Index
Velocity at 20 cm above bed (m/s)

C.

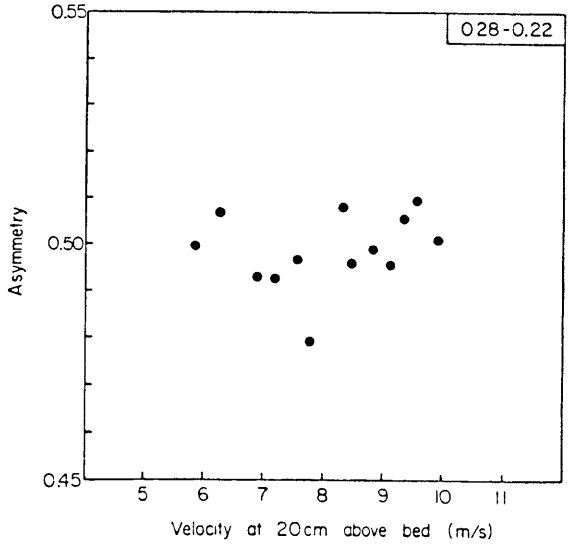
0.28-0.22
Asymmetry
Velocity at 20cm above bed (m/s)

D.

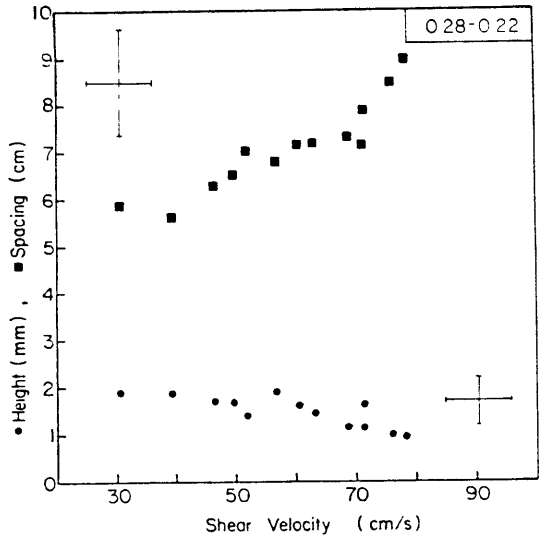
0 28-0 22
•Height (mm) , ■Spacing (cm)
Shear Velocity (cm/s)

E.

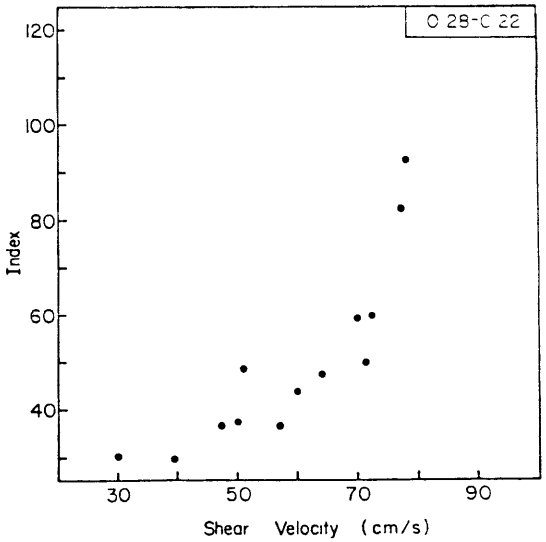
0 28-0 22
Index
Shear Velocity (cm/s)

F.

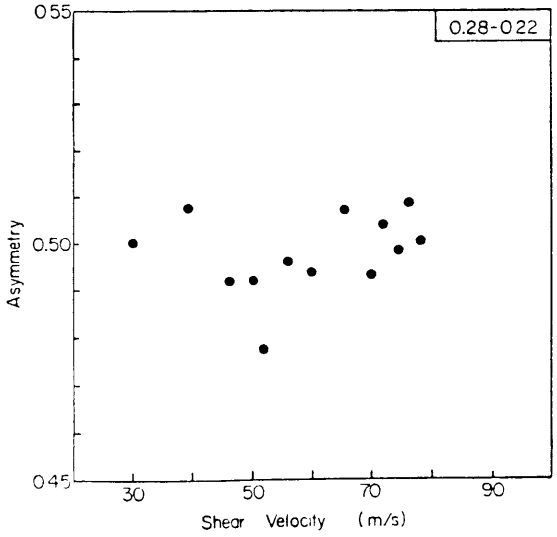
0.28-022
Asymmetry
Shear Velocity (m/s)

Figure 18. Morphology data for 0.20 mm sand. Error bars and plot labels the same as in Figure 9.

A.

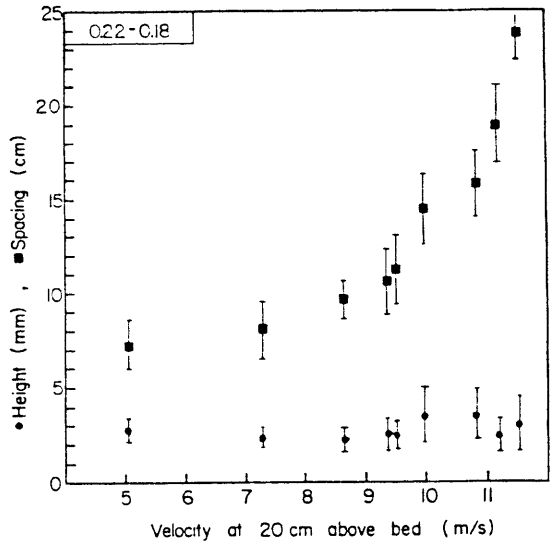
0.22-0.18
• Height (mm) , ■ Spacing (cm)
Velocity at 20 cm above bed (m/s)

B.

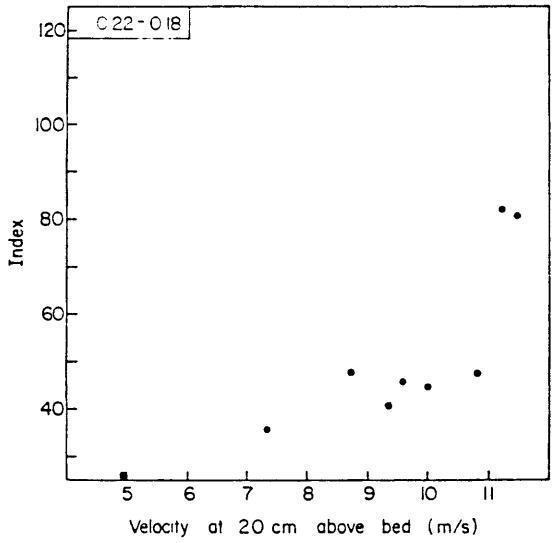
0.22-0.18
Index
Velocity at 20 cm above bed (m/s)

C.

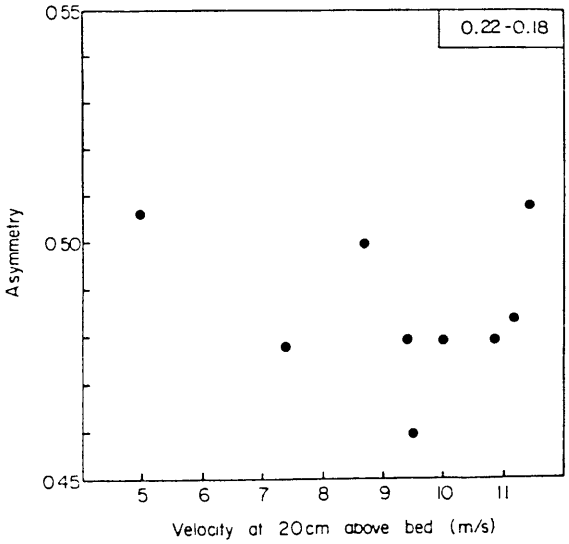
0.22-0.18
Asymmetry
Velocity at 20cm above bed (m/s)

D.

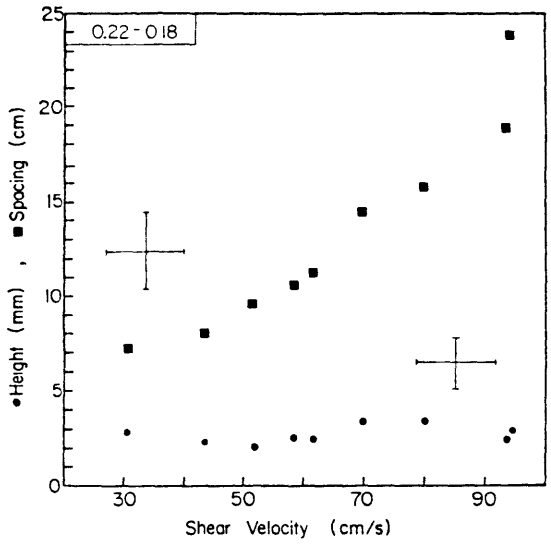
0.22 - 0.18
•Height (mm) , ■ Spacing (cm)
25
20
15
10
5
0
30
50
70
90
Shear Velocity (cm/s)

E.

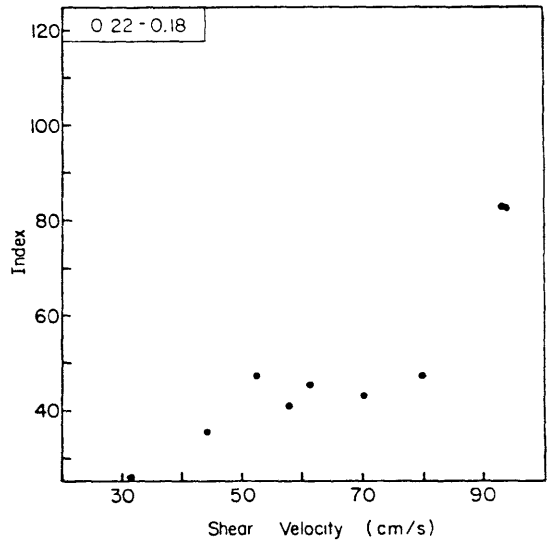
0 22 - 0.18
120
100
80
60
40
Index
30
50
70
90
Shear Velocity (cm/s)

F.

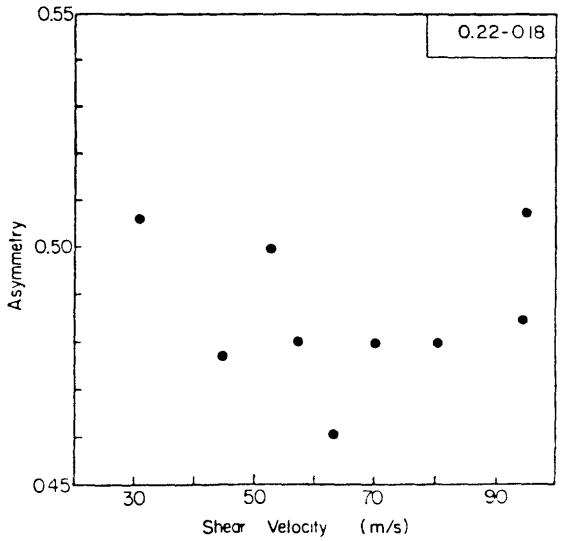
0.22-0.18
0.55
0.50
0.45
Asymmetry
30
50
70
90
Shear Velocity (m/s)

time to reach equilibrium, up to 15 minutes, and development time seemed to increase at higher velocities. The ripples in this sand appear to be markedly asymmetrical, and A was about 0.48 over much of the velocity range.

Sand D = 0.44 mm

Only spacing data were collected for this sand. Spacing increases at first with velocity, but at about U_{20} = 10.2 m/s there is a sudden sharp decrease (Figure 19). Below this velocity the ripples appear to be composed of non-saltating coarse grains that move only as creep (though this observation is unclear around the velocity where the change occurs, and is not experimentally documented at lower velocities since saltation load was not collected), and above this velocity coarse grain sizes also move in saltation.

Velocity Profiles

Wind velocity was measured at 1 cm, 3 cm, 5 cm, 10 cm, 15 cm, and 20 cm above the bed. To find U_* a linear-regression fit through all but the 1 cm velocity point was used to find the slope of the semilog curve of velocity versus height. As shown by Equation (2), this slope was multiplied by von Karman's constant (0.375) to obtain U_*. Resolution of a velocity focus was poor in these experiments, but a velocity defect is usually present, and is more pronounced at higher velocities (Figure 20). An explanation for the defect is that it is caused by the presence of saltating grains. That a focus was not clearly observed

Figure 19. Morphology data for 0.44 mm sand.

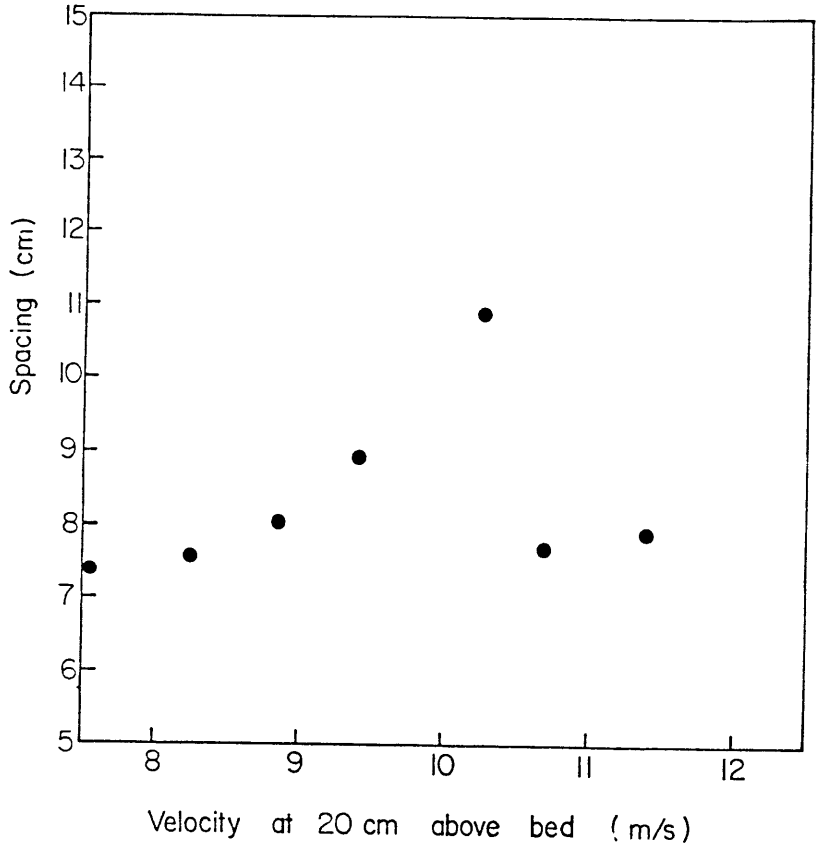
Spacing (cm)
15
14
13
12
11
10
9
8
7
6
5
8
9
10
11
12
Velocity at 20 cm above bed (m/s)

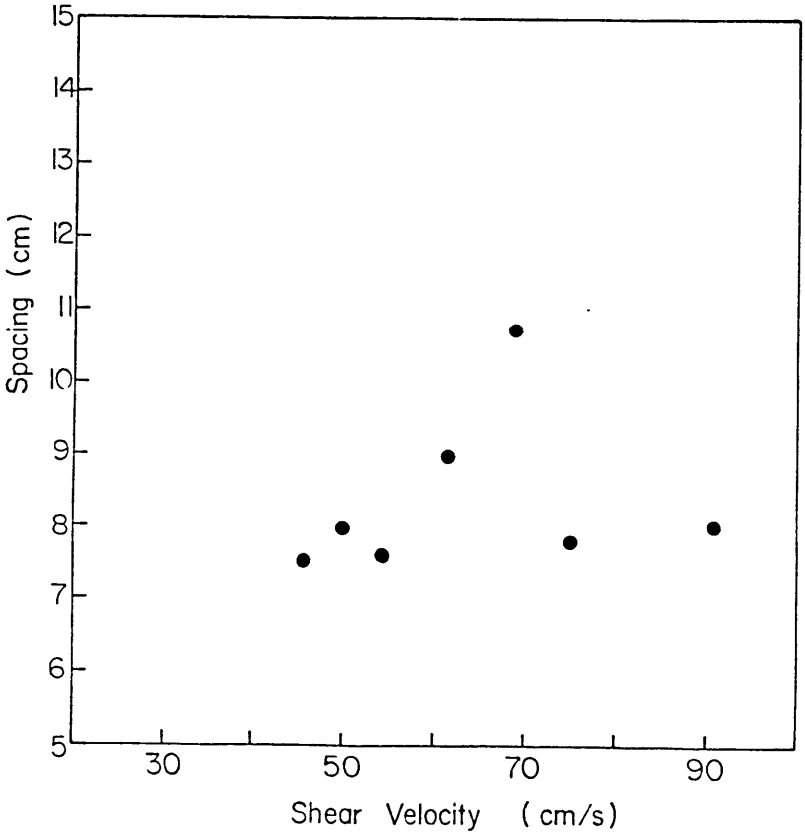
Spacing (cm)
15
14
13
12
11
10
9
8
7
6
5
30
50
70
90
Shear Velocity (cm/s)

Figure 20. Examples of velocity profiles measured in this study. Note the nature of the velocity defect and its change in magnitude with increasing velocity.

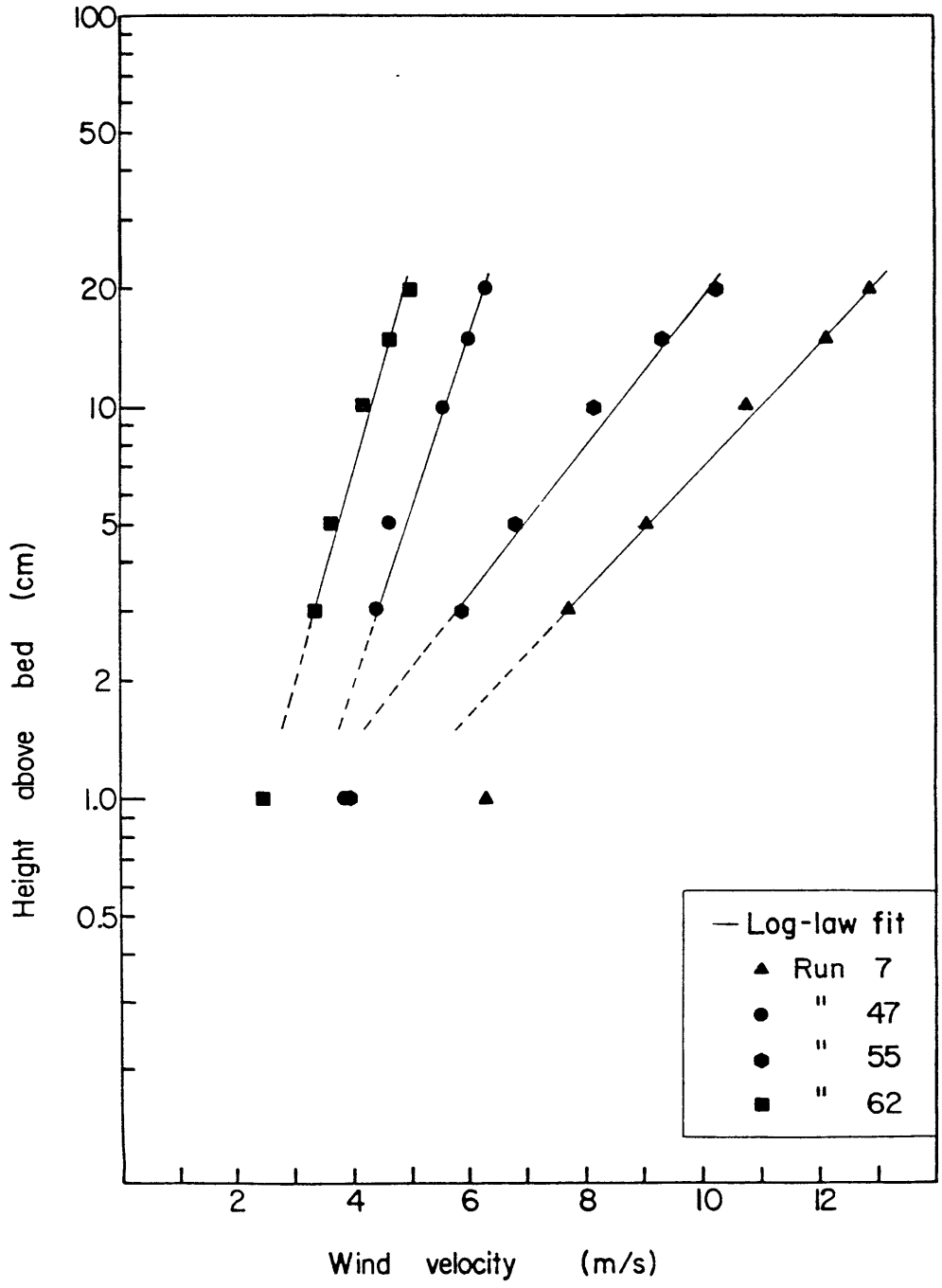
100
50
20
10
5
2
1.0
0.5
Height above bed (cm)
2
4
6
8
10
12
Wind velocity (m/s)
— Log-law fit
▲ Run 7
● " 47
● " 55
■ " 62

is to be expected, since Chiu (1972) demonstrated that the focus of the outer flow (above the saltation layer) is not well developed.

DISCUSSION

Ripple Morphology

The data presented above suggest that ripple morphology depends on wind velocity, mean grain size, and sediment sorting. We see from these data that for a given set of conditions, morphologic variables have a particular value. What follows is a discussion on how ripple morphology changes with sediment and flow parameters.

Over the mean size range of 0.78 mm to 0.32 mm a small variation in ripple spacing (less than 1 cm) for a given U_{20} is seen where the fields overlap (Figure 21). The ripples that form in the 0.78 mm sand have slightly larger spacing on average, but the variation is smaller than seen between 0.32 mm and 0.25 mm sands. This is not true of height; ripples in 0.78 mm sand are significantly larger than in 0.40 mm sand. Height at a given value of U_{20} decreases from the 0.78 mm sand to the 0.32 mm sand, and then increases radically in the 0.25 mm and 0.20 mm sands. Plots of height and spacing versus shear velocity exhibit slightly different trends. At a given value of U_* height and spacing decrease from the 0.78 mm to the 0.40 mm and 0.32 mm sands, then start to increase again in the smaller sizes (Figure 21). Clearly, ripple spacing and height not only increase with increasing grain size (as is generally accepted), but also increase in smaller grain sizes (below a size of about 0.32 mm) at a given value of U_*. Ripple spacing increases

Figure 21. Composite plots of ripple height and spacing against velocity at 20 cm above the bed and shear velocity.

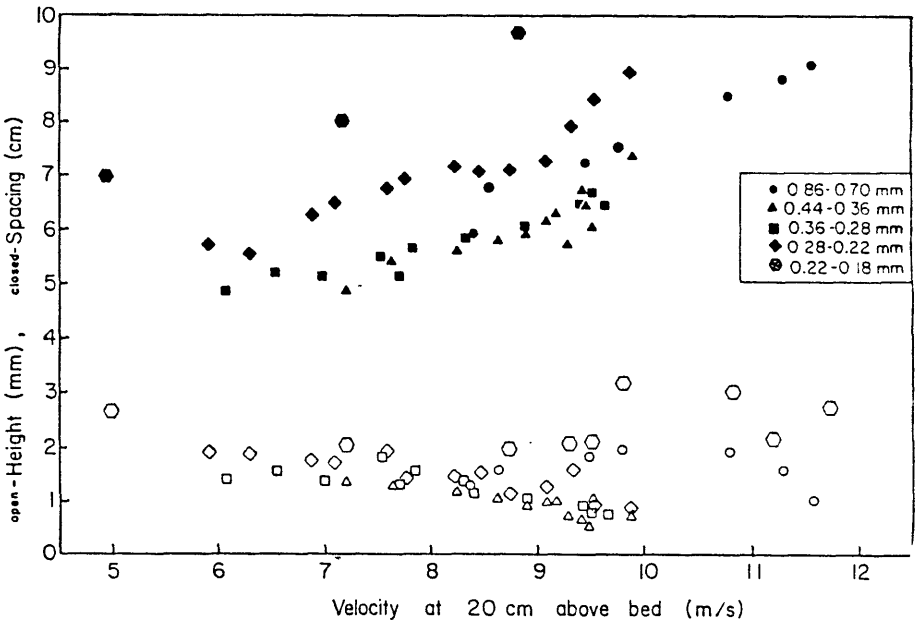
open-Height (mm), closed-Spacing (cm)
Velocity at 20 cm above bed (m/s)
0 86-0 70 mm
0.44-0 36 mm
0.36-0.28 mm
0 28-0.22 mm
0.22-0 18 mm

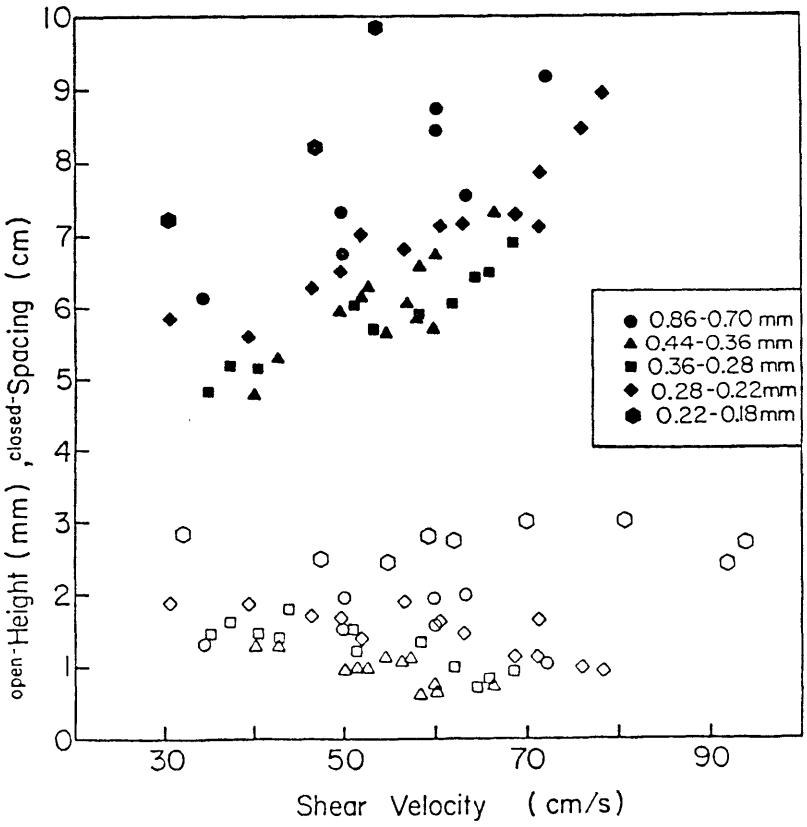
open-Height (mm), closed-Spacing (cm)
Shear Velocity (cm/s)
0.86-0.70 mm
0.44-0.36 mm
0.36-0.28 mm
0.28-0.22mm
0.22-0.18mm

with increasing velocity.

Since no clear trends in ripple asymmetry index are present, and since the ripples appeared to be quite symmetrical, ripple index I provides an accurate representation of the changes in ripple shape with velocity. High values of I indicate low relief, and low values indicate high relief. Index increases with velocity in all well sorted sands studied, except for the small initial decrease in the 0.78 mm sand at lower velocities. The plots of I versus U_{20} show that index is farily constant at lower velocities but increases drastically at higher velocities. Plots of I versus U_* typically show an increase in I over the entire range of velocities.

An important conclusion we can draw is that I increases strongly with increasing velocity. As the velocity increases the ripples flatten and lengthen (I increases), but the ultimate change to flat bed is farily abrupt ($I \to \infty$): the ripples stretch and flatten to a certain finite point, usually up to I = 80 or 100, then disappear with a small increase in velocity. This is true of all grain sizes in the well sorted sands. When we plot transition velocity against grain size we find that it decreases from 0.78 mm sand to the medium grain sizes, then increases again (Figure 22). If D = 0.44 mm sand (poorly sorted) were plotted, its transition value would lie well above the D = 0.40 mm sand, so sorting affects stability.

It is surprising that asymmetry index is so insensitive

Figure 22. Approximate velocities for transition to flat-bed transport.

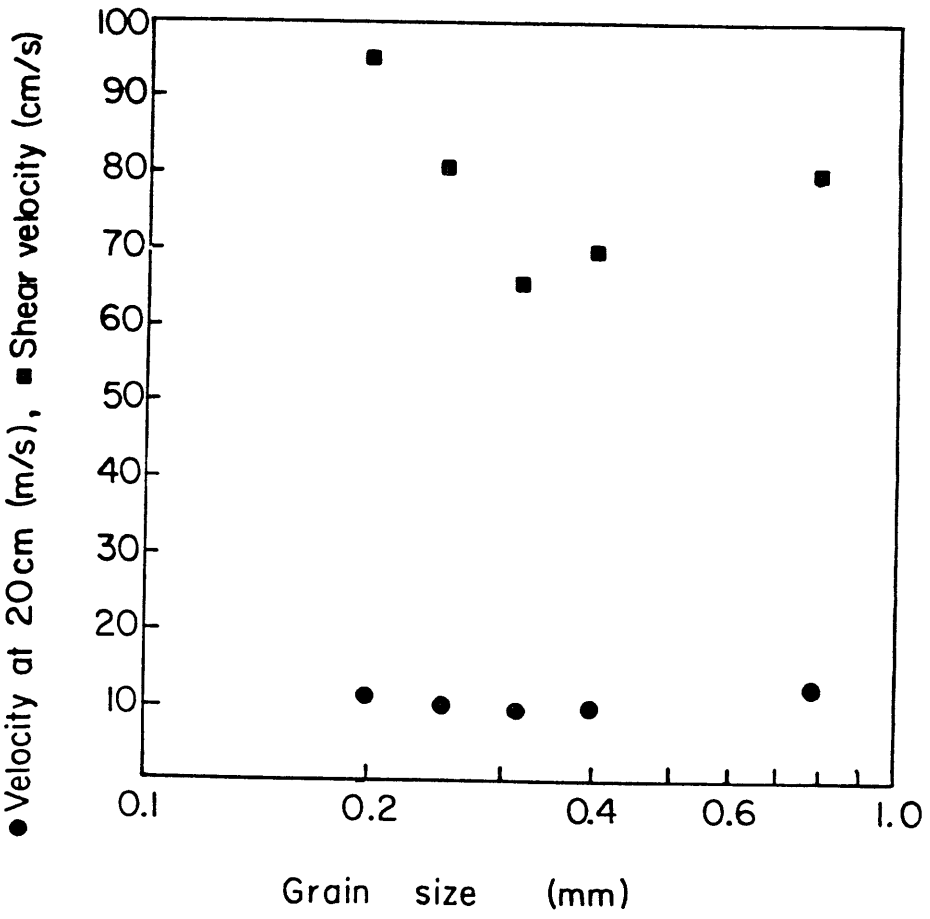
● Velocity at 20cm (m/s), ■ Shear velocity (cm/s)
100
90
80
70
60
50
40
30
20
10
0.1
0.2
0.4
0.6
1.0
Grain size (mm)

to changes in grain size and velocity: ripples in well sorted sands tend to be rather symmetrical ridges of sand, though ripples in 0.20 mm sand are somewhat asymmetrical.

The important difference between well sorted and poorly sorted sands are observed in the D = 0.44 mm sand: spacing can actually decrease with increasing wind velocity in poorly sorted sands; and between $\sigma \simeq 0.65$ spacing increases (assuming that the behavior of well sorted D = 0.44 mm sand is similar to D = 0.40 mm sand). The increased spacing (typically 2 cm) of this sand compared with sand D = 0.40 mm is seen only below $U_* \simeq 70$ cm/s in the region below the sudden decrease in spacing in the former. Above this value of U_* ripple spacing in D = 0.44 mm sand is comparable to that of D = 0.40 mm if we extrapolate the latter curve above its flat-bed value.

We should note from the discussion above that the plots of morphologic variables against U_{20} are different from those of U_*. These differences are quantitative and not qualitative: the general trends are similar, but the exact values are not the same.

Stone and Summers (1972) claim that ripple spacing is independent of velocity and sorting, but this seems untenable in light of the data presented above. If one examines the data presented by Stone and Summers (log-log plots of morphologic variables), the scatter present can easily accomodate any of the variations of spacing with velocity observed in this study. Unfortunately, their plots of

spacing versus sorting (expressed as standard deviation) give little information, because mean grain sizes are not provided. Variations of spacing with sorting at a given grain and velocity probably are sufficient to account for observed variation in these plots also. A plot of standard deviation versus spacing at a specific grain size would be interesting but not greatly helpful, as wind velocity is not considered. Thus, the finding that ripple spacing is a function of grain size alone is doubtful.

Characteristic Path

A formidable task is to deal with the present data in light of Bagnold's concept of characteristic path length and the findings of Ellwood et al. for mixed sizes. Bagnold assumed that the velocity profile he measured and the velocity profile kinks that he observed marked the average height of saltating grains, and then he computed a characteristic path for this height. His method is not given, but probably involved the susceptibility of sand grains to wind action (a concept of Bagnold's) and some sort of iterative calculation to find the path length. He found that the path length corresponded well to the measured spacing of the ripples. This correlation of mean path length and ripples spacing has been cited often in the literature. Using this concept, Ellwood et al. (1975) computed characteristic paths for bimodal sands and found that they could account for possible spacings of any ripple. However, they did not present any one-to-one comparisons of their values with values of actual ripples.

The conclusions of Bagnold and Ellwood, Evans and Wilson are unclear for the following reasons: (1) the velocity kink observed by Bagnold may be the result of insufficient data, and even if the data are complete enough, there remain doubts as to the nature of the velocity defect; (2) the mean path lengths obtained by other workers are significantly different from Bagnold's, and from observed ripple spacing; and (3) there is no a priori reason to think that the characteristic path length should correspond with ripple spacing, or that it should even exist as Bagnold defines it.

(1) As has been shown already (Figure 6), the nature of the velocity defect is unclear. When we examine other published velocity profiles, they all appear to be different near the bed. Bagnold found a negative defect with a kink at about 2 cm above the bed, but it can easily be argued that he had too few data to draw a log-law line. Kawamura (1951) found a similar type of profile (Figure 23). However, Zingg (1952) has a positive defect in his profiles (Figure 6) as does Belly (1964) on average (Figure 23). On the other hand, Horikawa and Shen (1960) show a negative defect. In the most complete study of velocity profiles in sand-transporting flows, Chiu (1972) always found a positive defect (Figure 24). From the profiles collected in the present study, defects are positive when present but are represented in the 1 cm velocity measurement only. Thus, the exact nature of a velocity defect is unclear but is

Figure 23. Sample velocity profiles from Kawamura (1951), Horikawa and Shen (1960), and Belly (1964).

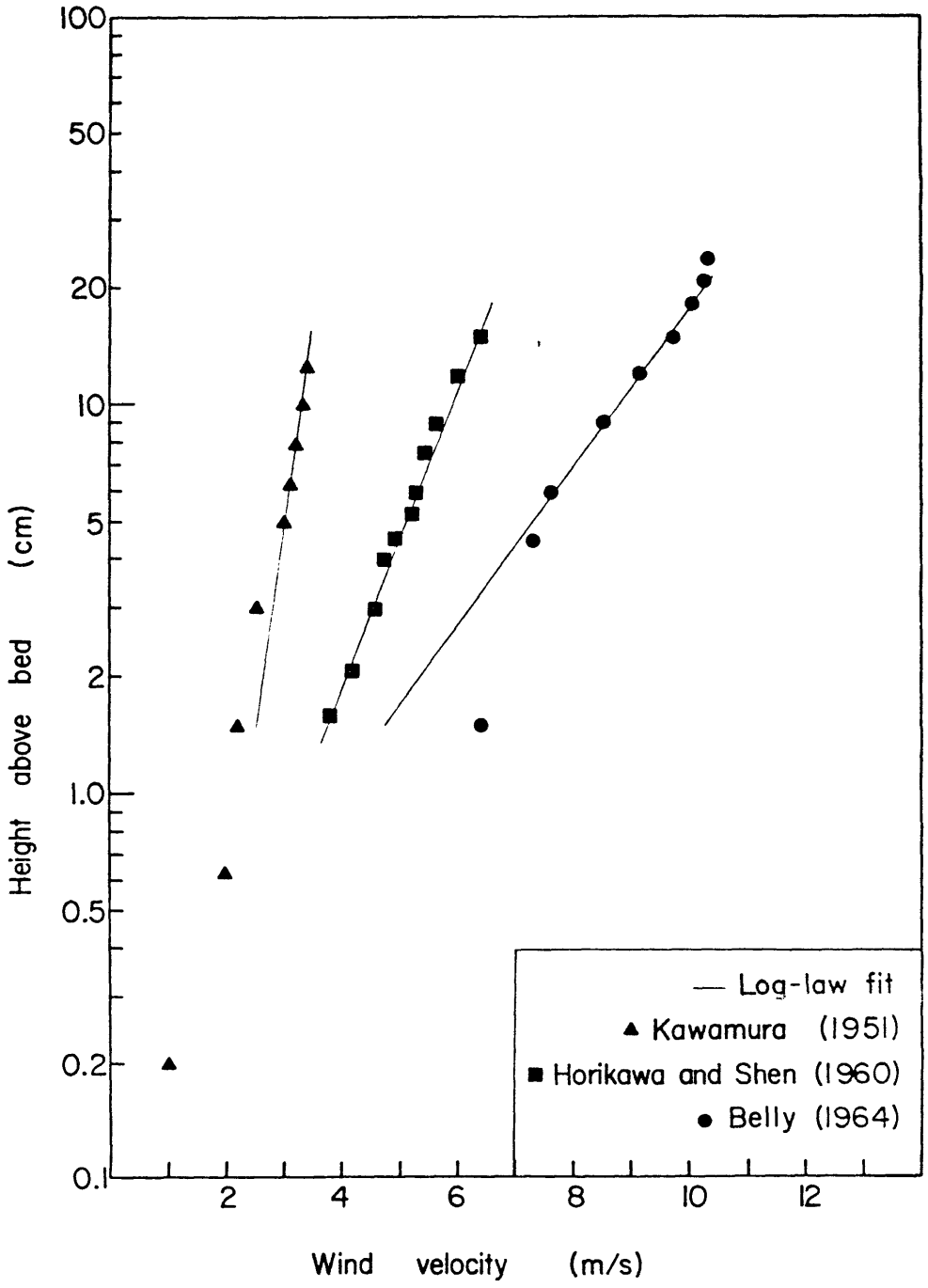
100
50
20
10
5
2
1.0
0.5
0.2
0.1
Height above bed (cm)
2
4
6
8
10
12
Wind velocity (m/s)
— Log-law fit
▲ Kawamura (1951)
■ Horikawa and Shen (1960)
● Belly (1964)

Figure 24. Sample velocity profiles from Chiu (1972). Note the nature of the velocity defect and the number of points that define it.

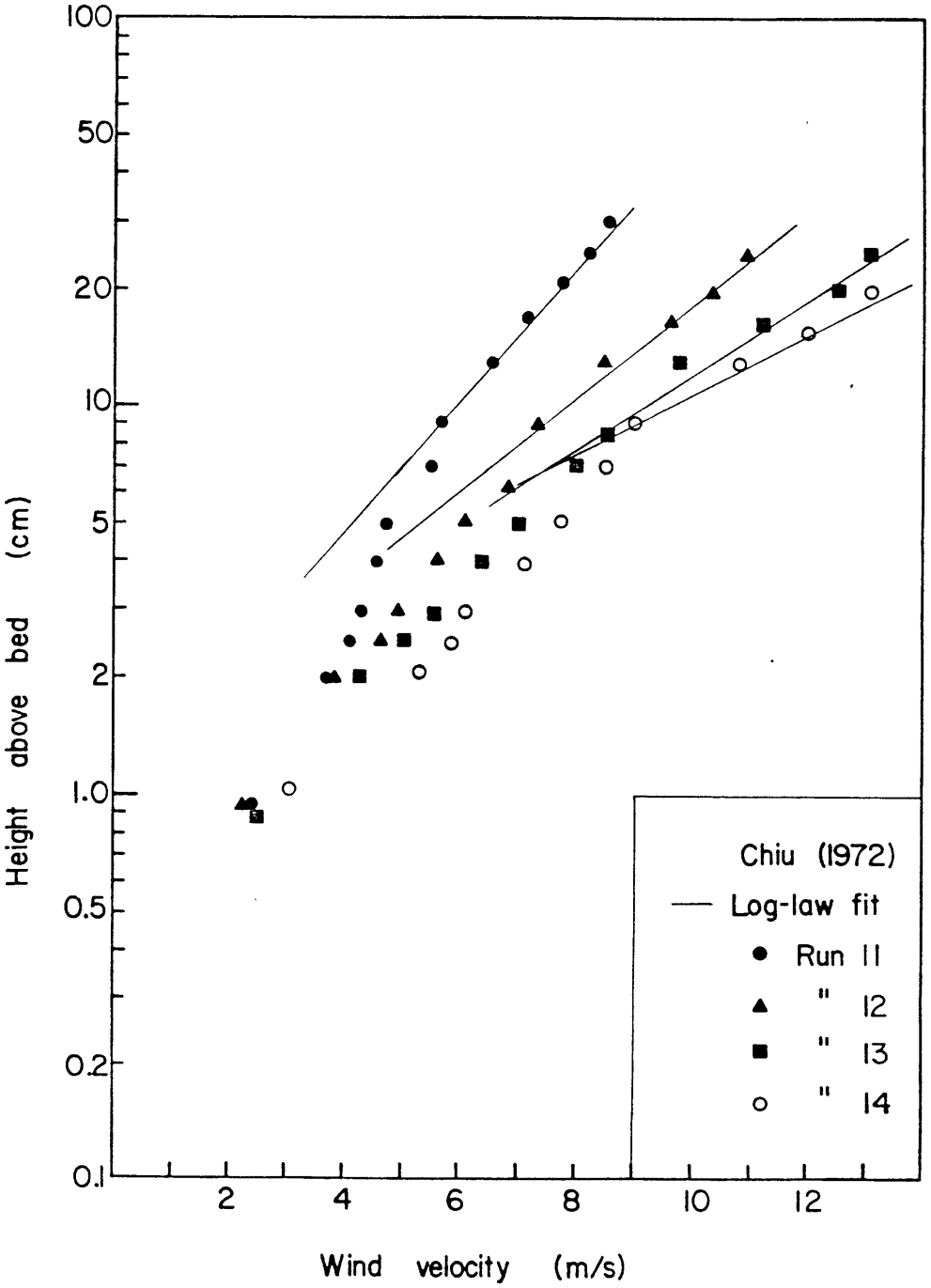
100
50
20
10
5
2
1.0
0.5
0.2
0.1
Height above bed (cm)
2
4
6
8
10
12
Wind velocity (m/s)
Chiu (1972)
Log-law fit
Run 11
" 12
" 13
" 14

probably positive (without a kink), as shown in the profiles of Chiu. Also, profiles that extend above 10 cm above the bed (Belly, Zingg, Chiu, this study) all have positive defects, and these profiles should be more accurate in defining a defect in the sense of Bagnold (defect from the log-law of the outer flow in the saltation layer) since they extend above the saltation layer. The only exception to this is the work of Horikawa and Shen (1960), but these authors drew their log-law fits to intersect at the point where the lowest velocity measurements clustered, and Zingg (1952) showed that a focus defined in this way does not coincide with the wall-law projections of measurements outside the saltation layer. We should also note that Bagnold assumed that the velocity focus coincided with the clustering of the points that are low in the velocity profile and not the projections of the velocity measurements outside the saltation layer. Chiu (1972) defined two foci: one from the log-law projection of measurements outside the saltation-affected part of the flow (poorly defined), and one from the log-law fit of data in the saltation layer. These foci do not coincide (see Chiu, 1972, for discussion).

(2) When we review the literature for values of the mean travel distance of saltating grains, we find little agreement among different authors (Figure 25). Bagnold's values were computed based on kinks in the velocity profile (which probably do not exist) and gives values between 1 cm and 27 cm (D = 0.25 mm). For a sediment with similar

Figure 25. Mean saltation distances computed by Kawamura (1951), Bagnold (1954), Horikawa and Shen (1960), and Belly (1964).

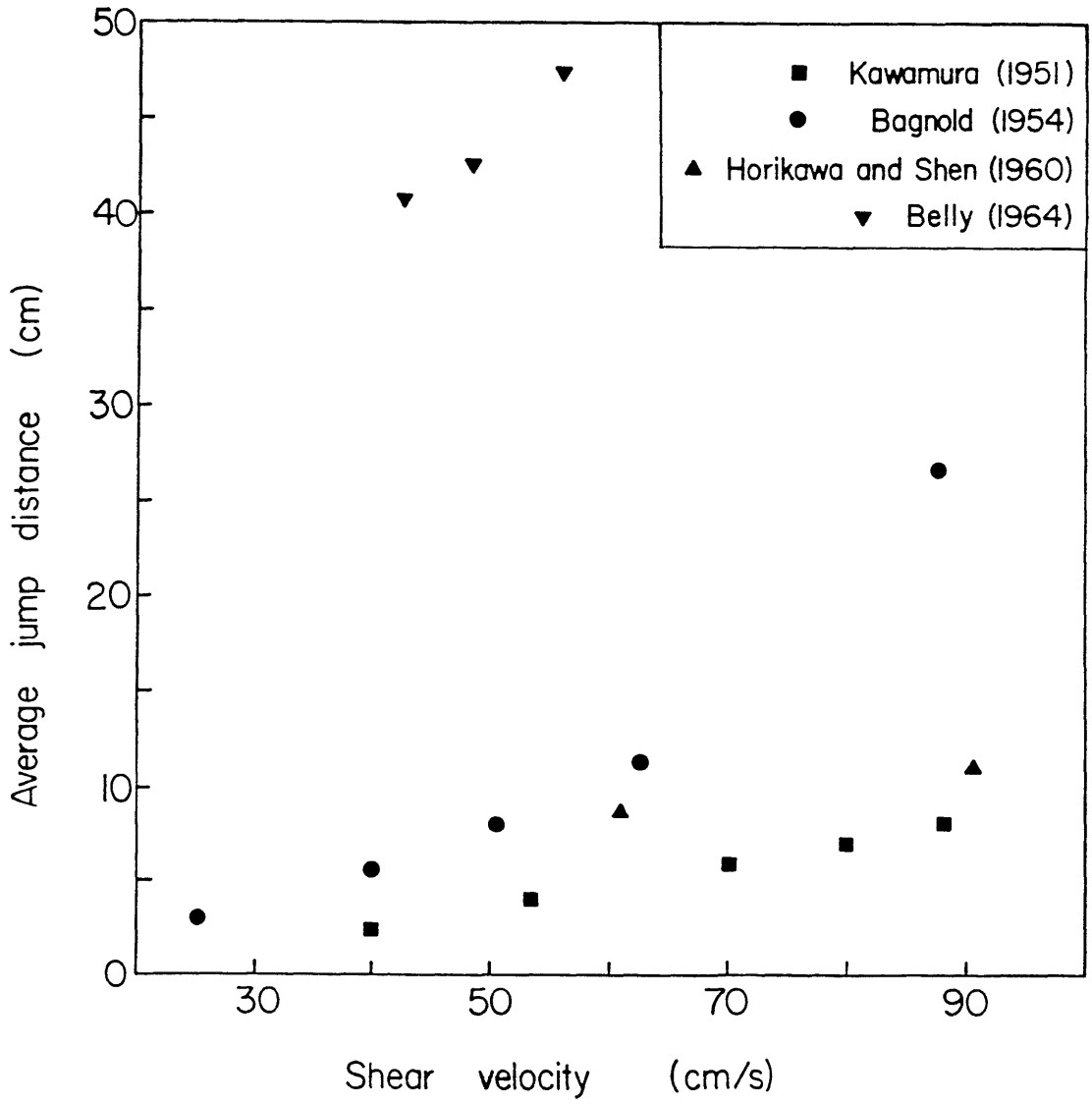
50
40
30
20
10
0
30
50
70
90
Average jump distance (cm)
Shear velocity (cm/s)
Kawamura (1951)
Bagnold (1954)
Horikawa and Shen (1960)
Belly (1964)

size, Kawamura found a smaller range of values (Figure 25). Belly computed jump distances of 30 cm to 50 cm, and Horikawa and Shen (1960) found values that were between those of Bagnold and Kawamura. Thus the conclusion that ripple spacing is the same as the mean jump distance of saltating grains is not well documented: we do not know what a true value for mean jump distance is.

(3) Throughout the literature on eolian bed forms, it is often cited that ripple spacing is equal to the length of the characteristic path of saltating grains. Sharp (1963) saw no reason why this must be true: from his analysis, summarized in the literature review above, he concluded that ripple spacing need not have anything to do with the mean jump distance of saltating grains. Sharp noted that sorting and grain size should be important since the ripple is composed of grains that move as creep. Bagnold mentions that spacing depends on path length, but height and shape depend on sorting. But by the arguments of Sharp, spacing depends on ripple height. In fact, while Ellwood et al. (1975) go to great lengths to show that all spacings found in eolian ripples can be accounted for by characteristic path alone, they completely ignored the effect of height on spacing (as did Bagnold). Flow separation does not occur over eolian ripples (Sharp, 1963), but something analogous to separation develops if the crest builds high enough and the lee slope is steep enough that saltating grains cannot strike grains on the lee slope. If this happens, few grains are

moved on the lee slope by saltation impact, so probably few grains in all are moved. A separation-like phenomenon of this sort can easily grow irrespective of the characteristic path length; in fact, this shadow zone might be important in megaripples. Thus, something more than path length must control ripple spacing. Indeed, even the concept of characteristic path as defined by Bagnold is difficult to accept. Bagnold claims that this characteristic path has dynamic significance: if all grains moved according to this path, the wind-velocity profile would be the same as in the natural case. The assumption that these two cases are similar is unclear. If the structure of the saltation layer changes from one that shows an exponential decrease of grain concentration with height to one that shows a constant concentration over a finite length, then the structure of the flow probably also changes, resulting in a different velocity profile. So whether the characteristic path as defined by Bagnold can even exist is doubtful. The writer attempted to formulate a characteristic path, similar to Bagnold's, and apply it to a velocity profile. But this sort of approach was found to be unrealistic, because knowledge of the Reynolds stresses is required. Owen (1964) assumed a mean path length and constant eddy viscosity, but such assumptions are ad hoc and cannot be treated seriously when small deviations from a constant value can cause large deviations in the velocity profile. The idea of a dynamic path exists mainly with Bagnold; path lengths computed by

others are merely mean jump lengths of grains in transport. Also inherent in the concept of characteristic path are kinks in the velocity profiles, which do not exist.

A point raised above is that height must also influence ripple spacing. Bagnold assumed that characteristic path controls ripple spacing, and that height is primarily a function of the sorting and size. Sharp demonstrated that height must affect spacing. A direct application of Bagnold's ideas that impact controls creep also supports this: a slightly higher ripple has a longer lee slope, and this slope is less affected by saltation impact, so that characteristic path can have little to do with controls on ripple spacing, but height does.

Sediment Transport and Ripple Morphology

As can be seen from the runs in this study in poorly sorted sediment and the work of Ellwood et al., the nature of the surface creep must be important. When creeping grains are composed largely of coarse grains that do not readily saltate, ripples grow larger (megaripples in the sense of Ellwood et al.) than when all grain sizes saltate (impact ripples). This change occurs with increasing velocity. But the velocity at which the coarse grains start to move is more than sufficient (with respect to U_* and U_{20}) to move even the coarsest grains in the mixture. Since saltation is a fluid shear phenomenon related in magnitude to U_*, we conclude that: the shear stress at the bed is

less than that predicted by the velocity profile of the outer flow; and that fluid shear at the bed increases with U_* of the outer flow. The first conclusion is not too surprising since probably not all of the energy required to support saltation comes from changes in eddy viscosity or in the viscous sublayer. However, the second conclusion is counter to the widely accepted notion that fluid shear at the bed is constant in sand-transporting flows. It should be cautioned that the changes in transport modes of coarse grains in poorly sorted sediment has never been demonstrated experimentally: it was first proposed by Ellwood et al. (1975) and is cited here as a possible explanation (i.e., not objectionable to the writer) for the morphologic behavior in poorly sorted sands. In all experimental studies of the saltation layer and the grain size distribution in it, no such change has been documented. However, these studies (Chiu, 1972; Williams, 1964) involved well sorted sand in which no such change would be expected or possible.

In both megaripples and impact ripples the bulk of the ripple translates as surface creep. The difference in morphology between the two ripple types depends on whether the grains that move as creep can also move as saltation. This dependence is primarily a function of grain size but also depends on sorting: in well sorted sands all grains saltate at all velocities above the threshold; in poorly sorted sand the ripples sort the fine grains to the troughs and into saltation, and the coarse grains move to the crest

of the ripple. This vertical sorting can be effective only above some certain unknown value of sorting for the bulk sediment mixture.

The process proposed by Ellwood et al. (1975) to explain the difference between impact ripples and megaripples, and suggested as a possible explanation for the behavior observed in the poorly sorted sand studied, must be reviewed critically. Megaripples are thought to form only in bimodal sands, but in this study they seemed to form in poorly sorted unimodal sediment. The process of saltation and creep suggested for megaripples is in a sense bimodal with respect to grain size. We could form this bimodal process in the following way. When transport begins at lower velocities, only the fine grains (up to a certain size) can be transported by saltation, and the other larger grains must creep: the fluid shear stress may be sufficient to move all sizes in the bed as saltation, but because of the presence of saltating grains, coarse material at the bed cannot saltate due to the lowering of the fluid shear stresses at the bed. This results in a bimodal process of saltation and creep with respect to grain size, much in the spirit proposed by Ellwood et al. (if not identical). The vertical sorting serves to further separate coarse grains from fine. At higher velocities all grains can saltate, so the bimodal process is not active: vertical sorting in the ripples still exists but is not as pronounced. These steps account for the observations of Bagnold and Ellwood et al.

In megaripples the ripple is composed of coarse grains that for the most part move as creep, and this is brought about by the ability of the ripples to sort fine material out of the coarse. It must be stressed that the above discussion is based on mechanical intuition and simple physics and has not been proven experimentally.

Mechanisms Controlling Ripple Morphology

We see from the discussion above that the nature of creep transport is poorly understood. Because of this poor understanding and the general poor understanding of eolian sand transport, our ability to formulate coherent arguments about the exact mechanisms involving sorting, wind velocity, and grain size to control ripple morphology is not good. We can formulate the following mechanisms:

(1) Ripples in poorly sorted sand have lower values of ripple index (build higher) by virtue of the concentration of coarse grains in the crest that allow the ripple to build higher at a given value of shear stress. The reasons for this are (a) the coarse grains are harder to dislodge by saltating grains, and (b) the coarse grains are more resistant to direct fluid shear.

(2) Creeping grains travel as creep over the length of their transport and are deposited in the lee face if the bombardment is not too great. Thus, at lower velocities the ripples should be able to build higher since creeping grains are not often pushed past the lee slope and crest

into the next trough.

This list is not long or extensive but realistically summarizes the known mechanisms that affect ripple morphology. Further speculations, such as the ripple spacing being governed by mean grain path or some function of grain size, have been shown to be tentative and based on little physical evidence.

Shear Structure and Impact Threshold

Many authors have proposed that the fluid shear stress at the bed is constant over all ranges of velocity when saltation is occuring. This idea is doubtful. We will critically examine the work of Kawamura (1951) and Owen (1964) to determine whether the fluid shear at the bed is constant.

Eolian transport at velocities suitable for ripples typically occurs in two modes: saltation and creep. However, the physics of grain interactions when they are in the saltation mode or in the saltation and creep modes is not well formulated (if at all). But any model involving shear-stress distribution must be related to grain transport, since shear stress at the bed is distributed between grains and fluid. Our understanding of particle motion consists of (1) arguments for forces acting on a grain at the bed and how it is lifted into saltation (Bagnold, 1954; Zingg, 1952; White and Scholz, 1977; and Tsuchiya, 1970), and (2) arguments for forces acting on a grain while it is in saltation.

We have no good theoretical or empirical understanding of particle interactions (except Bagnold, 1956), but discussion and treatments of the authors above (Owen, Kawamura) deal with stress distribution and flow structure, ignoring the physics of grain interactions.

Kawamura (1951) presented the following argument for constant fluid shear stress at the bed; call the mass of grains falling into a unit area per unit time G; let G' be the mass of grains in this area that never jump again after striking the bed; let G" be the mass of grains newly moved by the wind. Further, assume that:

$$\tau_0 = \tau_s + \tau_w$$
$$G' = aG$$
$$G'' = b(\tau_w - \tau_t)$$

where

a = constant

b = constant

τ_w = wind stress at the bed

τ_t = critical stress (fluid threshold)

τ_s = shear produced by saltating grains

(c = constant), $\tau_s = cG$

At equilibrium it can be demonstrated that:

$$G = b(\tau_0 - \tau_t)/(bc + a)$$

(see Kawamura, 1951). From this relation we find:

$$\tau_s = bc(\tau_0 - \tau_t)/(bc + a)$$

then

$$\tau_w = \tau_0 - bc(\tau_0 - \tau_t)/(bc + a) \qquad (3)$$

Kawamura then states that in a fully developed transport profile, grains that rest after collision are few, so $a \to 0$. Thus:

$$\tau_w = \tau_t$$

But for continuity of sediment transport, if $a \to 0$, then b must also go to zero (if all grains that move continue to move, then for constant G no new grains can move, thus $b \to 0$). So, the right-hand side of Equation (3) is the indeterminate form 0/0, and we do not know what it approaches in the limit. Thus, the conclusion that $\tau_w = \tau_t$ is wrong.

Owen (1964) presented another argument for fluid shear stress at the bed remaining constant over the range of applied flow shear stresses when sediment is in transport. Again, one of the basic assumptions is that the bed shear stress can be divided between the flow and the saltating grains. Owen states that fluid shear at the bed is constant at the value of the impact threshold. Impact threshold was observed by Bagnold (1954) and is the threshold for grain transport (by saltation) if grains are dropped onto the bed from above. The impact threshold occurs at lower values of flow shear stress than the fluid threshold: impact

threshold = 0.64 (fluid threshold). Owen and Bagnold assume that the impact-threshold transport is stable, that is, is indefinitely continuous downwind. Owen states that this value of fluid shear stress is just sufficient to ensure that the bed is in a mobile state and that the added energy by saltating grains is enough to continue saltation. The reasoning for this assumption is that if the fluid stress at the bed rises above the impact threshold, the bed is eroded, with more grains put into transport. In fact, grains are put into transport until the concentration is adequate to lower the fluid shear stress at the bed to the value of the impact threshold. The assertion that the fluid shear at the bed is constant at the value for impact threshold is a contradiction of the basic assumption that the total bed shear stress is divided between the grains in saltation and the fluid.

If the fluid stress at the bed is constant at the threshold value, then when stable transport begins at this value, the fluid stress at the bed must drop, since grains in the flow are assumed to take up part of the bed shear stress. In other words, the assumption that the shear stress at the bed is composed of a fluid and grain input and that the fluid shear at the bed is constant at the value for impact threshold (regardless of the applied shear stress if transport is occurring) are contradictory if transport occurs (and it does) at the impact threshold, since the applied shear stress from the outer flow and fluid shear stress at

the bed must be equal (leaving nothing for the saltation of grains). So we see that the fluid stress cannot be constant at the value for impact threshold. The argument presented above for fluid shear stress changing with velocity in poorly sorted sands also contradicts the hypothesis of constant fluid shear stress.

It could be argued that, because saltating grains strike the bed and appear to rebound back into the flow, lift forces are not acting on them, rather it is really an elastic rebound. The word "appear" is important here, since, to the writer's knowledge, no detailed observations at the bed have been made during sediment transport. White and Scholz (1977) have come the closest to observing bed processes, though they admit that study close to the bed is not possible because of the high concentration of particles. They state, however, that it is possible for saltating grains to help eject other grains (process unknown), to bury themselves, or to rebound. With all of these possibilities, it seems clear that increased lift at the bed (implying increasing fluid stresses at the bed) must operate, or insufficient numbers of grains would be put back into the flow after saltation impact.

What is the significance of the impact threshold, and is it uniquely defined? Impact threshold is the value of bed shear stress for which artificially induced saltation will continue but will not occur without added input. In relevant wind-tunnel studies (Chepil, 1945; Bagnold, 1954)

grains were dropped through the flow from the top of the wind tunnel, struck the bed, and a saltation layer was observed to develop. We might assume that the accelerated grains from the roof provide the added energy at the bed to cause saltation. Therefore, the impact threshold might be dependent on tunnel height. Impact threshold has been studied only in wind tunnels of square cross section that were relatively short (less than 10 m). This might introduce error in two ways: (1) because of the square cross section, secondary circulations will be strong and will cause areas of anomalously high shear stress at the bed that could cause transport, or might aid in perpetuating artificiallly induced transport; and (2) because of the short lengths, documentation of impact threshold continuing indefinitely downwind is not good, since longer distances might be required for transport to cease. In regard to the second point, at shear stresses below impact threshold, saltation occurs over short distances when artificially induced, so as shear stress increases, it probably requires longer and longer distances for transport to cease. It is possible that transport might stop at the given value of impact threshold given a sufficient tunnel length. A limiting value for shear stress for stable transport should be the fluid threshold. These concerns are real and unanswered in previous and present studies but should be fully dealt with before any serious applications of the impact threshold should be attempted.

But these comments only detract from previous ideas of shear-stress structure and add few alternatives. What follows is a discussion that attempts to relate physics qualitatively to transport problems. When grains saltate, they leave the bed at high initial angles (40° to 60° on average). This indicates that lift rather than elastic rebound is causing the grains to leave the bed. Owen (1964) observed that the height of the saltation layer depends on U_*, in fact $H = U_*^2/g$. Since lift forces on a grain are also functions of U_*, this indirectly indicates that lift forces control the height that grains attain and are responsible for initiating saltation. If this is true, then the increased number and height of grains in saltation at higher U_* can be viewed as the increase of lift forces at the bed, and the effect of saltating grains to dislodge bed grains so that they are easier to transport. This is not to say that grain rebound and successive saltation do not exist and are unimportant. Rather, this simply means that the fluid shear at the bed increases as some proportion of U_* and is responsible for the height of the saltation layer and the increased number of grains in transport. This writer feels that lift forces must be acting on the bed, because (as stated by Owen) saltating grains can impart only horizontal momentum to the bed grains.

We should remember that since grains leave the bed at high angles some forward momentum is taken from the fluid near the bed, but horizontal translation of grains results

primarily from their interaction with the flow in the higher part of their trajectories. But as the grains approach the surface, they impart momentum back to the lower part of the flow, and probably a greater amount than is extracted from this region when the grains initially rose. Thus, the positive defect observed in the velocity profile might be the result of the grains putting momentum back into the flow. It could also be caused by changes in the Reynolds stresses due to the presence of the grains. It has been shown in water (Gust and Southard, in press) that von Karman's constant is significantly lowered at the bed when grains are in transport. If this is true for air, then we might be seeing a double boundary-layer structure: the lower part of the slatation layer has drag reduction and a higher U versus z slope; and the upper part of the flow is a rough-wall flow that is responding to the saltation layer as a roughness height.

Development of Transport

A major concern in eolian studies is that the transport profile be fully developed at the point of measurement. Belly (1964) noted a lower-than-expected transport rate at his measurement point in preliminary work, but found that by introducing sediment into the flow at the upstream end of his sand bed, equilibrium sand transport was quickly obtained downwind of the point of introduction. The same phenomenon was observed by Bagnold (1954). Kawamura (1951)

concluded that transport was fully developed after only 2 m of tunnel length, but Bagnold indicates that at least 5 m are required in 0.18 - 0.30 mm sand when no sediment is fed into the flow.

In this study an exploratory set of runs was made to ascertain the distance needed for development of transport. These runs were made using 0.78 mm sand, and the results have been qualitatively described above. The experimental set-up is shown in Figure 26, and the results in Figure 27. The large deviations in "equilibrium" transport quantities are caused by the poor design of the sand traps, but rough qualitative estimates can be made. Development distance is great in runs without sand feed, and full development is not obtained in the 15 m. When sediment is introduced, the first two sand traps record high transport, but the others are essentially the same (within possible error). At higher velocities without feed, transport develops more quickly but still not completely down the tunnel. When the flow was drastically overfed (at high velocity), the first two traps have larger than equilibrium deposition, but transport is fairly constant past 7 m from the sand feed.

Threshold Values

As most recently summarized by Miller et al. (1977), values of shear stress for transport obtained in eolian studies are low when plotted on a Shield diagram. One factor that might greatly contribute to this is the tunnel shape

Figure 26. Experimental arrangement for studying transport profile. Note position of sand feed relative to the sand bed, and the positions of the sand traps relative to the sand feed.

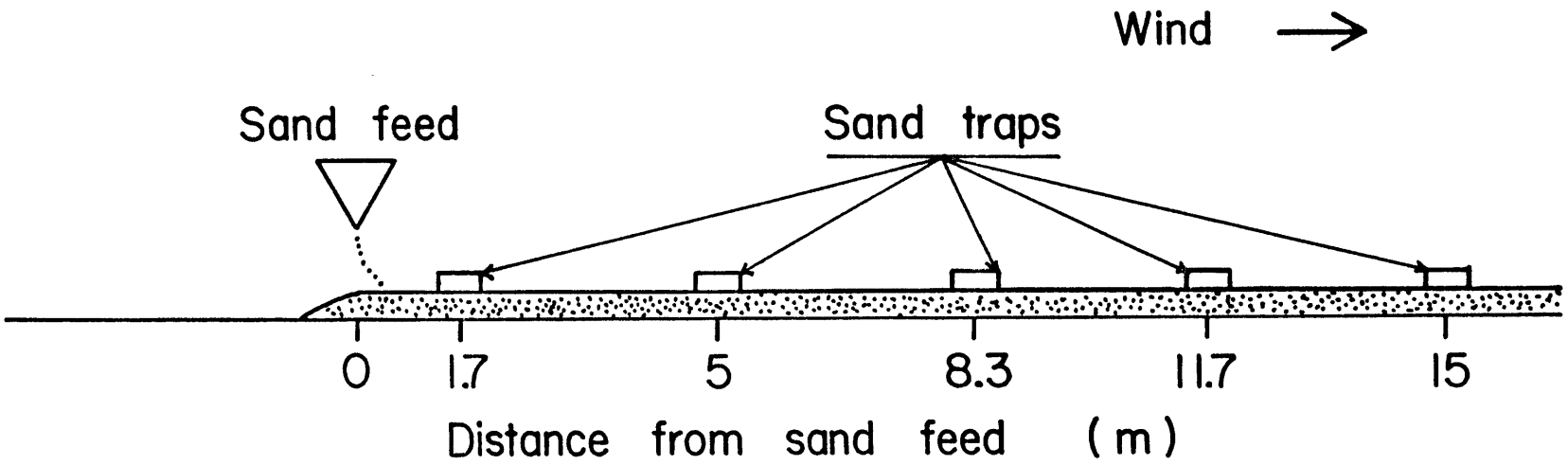
Wind
Sand feed
Sand traps
0
1.7
5
8.3
11.7
15
Distance from sand feed (m)

Figure 27. Results of the experiments of the development of the sand transport with distance down the tunnel.

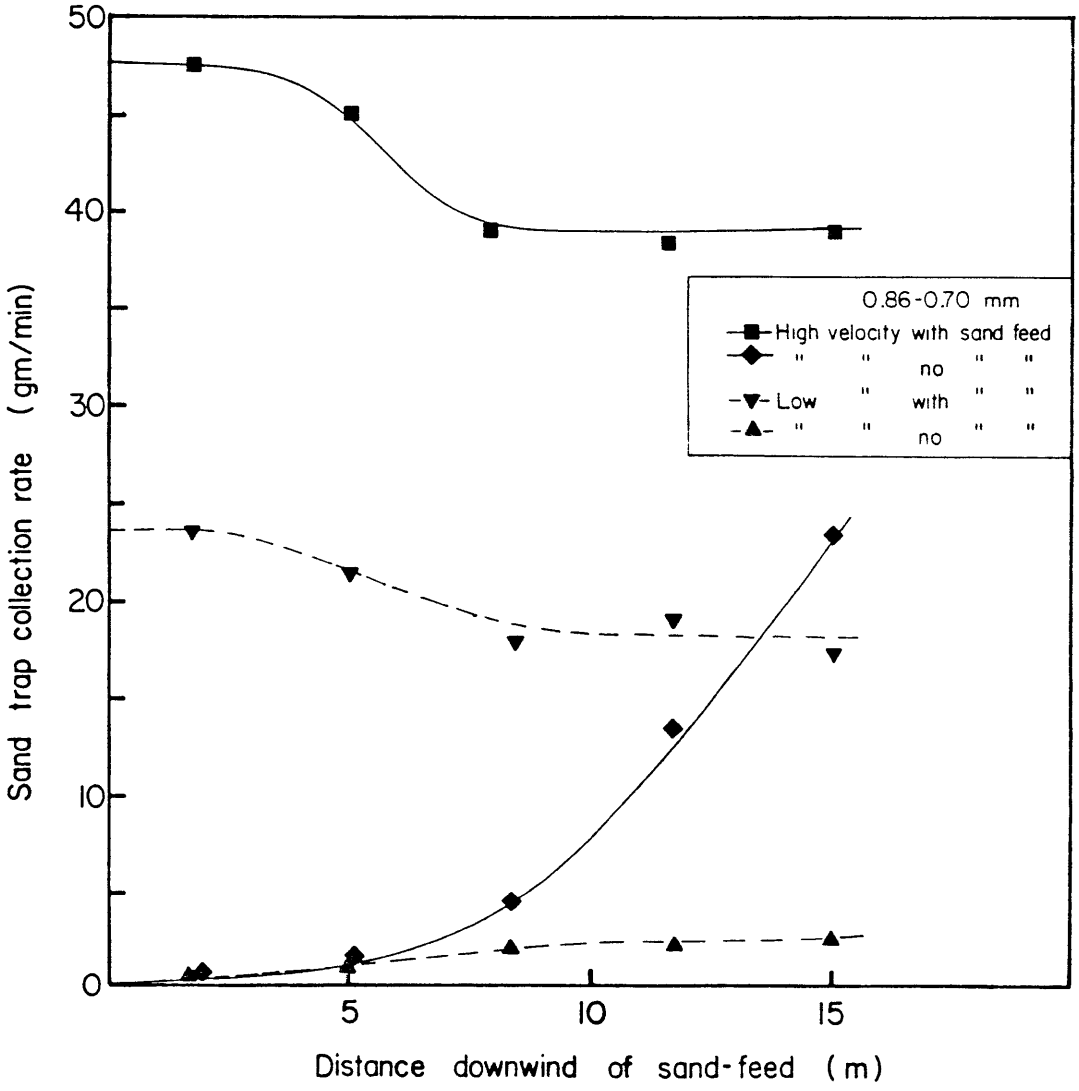
50
40
30
20
10
0
5
10
15
Sand trap collection rate (gm/min)
Distance downwind of sand-feed (m)
0.86-0.70 mm
High velocity with sand feed
" " no " "
Low " with " "
" " no " "

used by most previous workers (Zingg, 1952; Bagnold, 1954), in that their tunnels have width/height ratios of unity. This sort of configuration leads to the development of strong secondary circulations which cause abnormally high shear stresses at the bed. In this way we might explain this discrepancy. It could be argued that Zingg computed his threshold values not from observation of the bed but by the intersection of his curves of shear stress plotted against fan pressure for those runs where transport did occur and those over a fixed bed, thus reflecting only the true bed shear stress for transport. However, a scan of Zingg's data shows scatter and trend lines that do not reflect the data, so his values are questionable. Thus, a clear picture of threshold values for eolian transport does not exist.

Vertical Sorting in Ripples

To investigate vertical sorting produced in poorly sorted sands, several ripples were sectioned for size analysis. The ripples were wetted with water then physically removed from the wind tunnel. The crests, underlying carpet, and undisturbed original material were separated, the sand was allowed to dry, and then a size analysis was made. The results are shown in Figure 5.

Two striking features are present: the crest consists of considerably coarser material than the original bed; and the carpet of ripple-worked material is slightly enriched in fines relative to the original bed. Examination reveals that

the carpet is somewhat enriched in heavy minerals compared with both the crest and the original bed. These results are similar to those of Zingg (1952). So the layer of fines observed by Sharp (1963) can be produced by ripple action and does indeed represent working and sorting of the bed material by the ripples.

Mathematical Treatment

Kennedy (1964) presented a detailed and informative stability analysis of the wind ripple problem. His approach, however, has a major shortcoming; he assumed that a transport lag distance existed. We will attempt to analyze the ripple problem without using a lag distance.

Wind ripples move primarily as creep, that is, the grains composing the ripple generally move as creep under the impact of saltating grains. Recognizing this fact, we can disregard the explicit use of wind-velocity variation over the ripple and examine only the influence of saltation. Bagnold (1954) presented a relationship between the surface slope and the intensity of creep (assuming a constant impact angle for saltating grains). Fortunately, this relation is approximately linear over most of the ripple ($-10° < \text{surface slope} < 20°$). We start with the sediment continuity equation:

$$\frac{\partial h}{\partial t} + a \frac{\partial q}{\partial x} = 0 \qquad (4)$$

where

h = height of bed form above zero datum

a = constant that incorporates porosity

q = sediment transport

From the discussion above, we can postulate that q is a function only of the surface slope. Thus:

$$q = f(\frac{\partial h}{\partial x}) \tag{5}$$

More specifically:

$$q = m + md(\frac{\partial h}{\partial x})$$

where

m = transport rate over a flat surface

d = limiting angle so that $q \to 0$ when the lee slope is parallel to the impact angle

So Equation (4) becomes:

$$\frac{\partial h}{\partial t} + M(\frac{\partial^2 h}{\partial x^2}) = 0 \tag{6}$$

where

$M = \partial md$

We will now introduce a small perturbation into the equation and solve the temporal problem. Let $h = H_o + h_o$, where H_o is the original bed profile and h_o is the perturbation. Let h_o be of the form:

$$h_o = \varepsilon/k(e^{i\theta}) \qquad (7)$$

where

$$\theta = k(x - ct)$$

$$k = 1/L$$

$$c = c_r + ic_i \text{ (ripple velocity)}$$

$$\varepsilon = \text{perturbation height (dimensionless)}$$

Equation (6) becomes:

$$\frac{\partial H_o}{\partial t} + \frac{\partial h_o}{\partial t} + M\left(\frac{\partial^2 H_o}{\partial x^2}\right) + M\left(\frac{\partial^2 h_o}{\partial x^2}\right) = 0$$

Since H_o is fixed in time:

$$\frac{\partial h_o}{\partial t} + M\left(\frac{\partial^2 H_o}{\partial x^2}\right) + M\left(\frac{\partial^2 h_o}{\partial x^2}\right) = 0 \qquad (8)$$

Substituting Equation (7) into (8) and collecting terms of order ε we find that:

$$c_i = kM$$

$$c_r = 0$$

Since k and M are always greater than zero, this result implies that all disturbances grow but do not translate.

Thus, the assumption that surface slope alone controls creep rate is insufficient to lead to a meaningful characterization of ripples. Let a further assumption be that q also depends on ripple height. This is reasonable

since shear stress over the ripple should vary with height, and this variation will cause a differential amount of sediment to move by direct fluid shear. So we assume that:

$$q = M\frac{\partial h}{\partial x} + Sh$$

where S is a positive constant. Thus, by substitution, Equation (4) becomes:

$$\frac{\partial h_o}{\partial t} + M\frac{\partial h_o}{\partial x^2} + M\frac{\partial^2 H_o}{\partial x^2} + S\frac{\partial^2 h_o}{\partial x_o^2} = 0$$

Solving to order ε:

$$c_r = kS$$

$$c_i = kM$$

Since all these quantities are positive, this solution predicts that all disturbances grow and translate. Neither of these approaches is successful in predicting ripple morphology, e.g., predicting spacing or velocity. Thus, the simple physically justified assumptions are not sufficient. This writer did not push past this step, because further assumptions make the equations mathematically intractable and in any case are not justified by observation of sand transport over ripples and thus would be introduced for analytical and not physical reasons.

CONCLUSIONS

Ripple spacing increases with increasing wind velocity in well sorted sands. The increase of spacing with velocity is qualitatively similar in sands with a mean size between 0.25 mm and 0.78 mm, but is much more rapid in sand with grain size of 0.20 mm. Runs in poorly sorted sediment show that ripple spacing can decrease, albeit discontinuously, with increasing velocity, although above and below the discontinuity spacing increases with velocity. The discontinuity occurs when the transport mode of the coarest grains changes from all creep to a combination of saltation and creep. Values of spacing increase with increasing grain size above a mean grain size of 0.32 mm, and also increase with decreasing grain size below 0.32 mm.

Ripple height decreases as wind velocity increases, except at velocities close to the threshold value, where height is fairly constant or may actually increase. In the finest sand studied the variation of ripple height with velocity was irregular

Ripple index increases with increasing velocity. Index increases to a certain finite value, I = 80 or 100, near the velocity for flat-bed transport, and becomes infinite as ripples disappear with a small increase in velocity. Velocity for flat-bed transport decreases from large grain sizes down to the 0.32 mm sand, then increases in the smaller sands; for a given mean grain size it also increases as the sand becomes less well sorted.

Ripple asymmetry did not exhibit distinct trends in the well sorted sands, with the exception of the 0.20 mm sand. Asymmetry index in that sand was constant at about 0.48, and ripples were markedly asymmetrical. In the other well sorted sands ripples were symmetrical.

Ripple spacing is not equal to the characteristic path length of saltating grains. Characteristic paths computed by Bagnold (1954) are incorrect, because (1) kinks in the velocity profile do not exist and thus cannot mark the average height of saltating grains, and (2) a characteristic path as defined by Bagnold does not exist. Path lengths computed by other workers do not correspond to actual observed values of ripple spacing.

Ripples grow higher in poorly sorted sands. Vertical sorting of coarse grians to the crests of ripples causes the crests to build higher. At low velocities ripples grow higher, because crestal grains are not as easily propelled past the lee slope into the downwind trough.

The bed shear stress is divided between the fluid and saltating grains. The amount borne by the fluid is not constant, but increases with increasing velocity. The shear velocity measured outside the saltation layer is the total shear input into the saltation layer and the bed. The shear velocity measured in the saltation layer has no clear relationship to shear structure or energy transfer in the flow system.

REFERENCES

Bagnold, R.A., 1954, The Physics of Blown Sand and Desert Dunes: Chapman and Hall, London, 265 pp.

Bagnold, R.A., 1956, The flow of cohesionless grains in fluids: Proc. Roy. Soc. A, 249, p. 235-297

Batchelor, G.K., 1967, An Introduction to Fluid Dynamics: Cambridge Univeristy Press, New York, 615 pp.

Bateman, H., 1944, Partial Differential Equations of Mathematical Physics: Dover Publications, New York

Belly, P.I., 1964, Sand movement by wind: U. S. Army Corps of Engineers, Technical Memorandum No. 1, 38 pp.

Blatt, H., Middleton, G.V., Murray, R., 1972, Origin of Sedimentary Rocks: Prentice-Hall, Inc., New Jersey, 634 pp.

Borowka, R.K., 1980, Present day dune processes and dune morphology on the Leba barrier, Polish coast of the Baltic: Geograficka Annaler A, 62, p. 75-82

Buckingham, E., 1914, On physically similar systems; illustrations of the use of dimensional equations: Phys. Rev., 4, p 345-376

Carrol, D., 1939, Movement of sand by wind: Geol. Mag., 76, p. 6-23

Chepil, W.S., 1945, Dynamics of wind erosion: II. Initiation of soil movement: Soil Science, 60, p. 397-411

Chepil, W.S., 1958, The use of evenly spaced hemispheres to evaluate aerodynamic forces on a soil surface: Trans. Amer. Geoph. Union, 39, p. 397-404

Chiu, T.Y., 1972, Sand transport by wind: Dept. of Coastal and Oceanographic Engineering, Tech. Report No. 1, 53 pp.

Cornish, V., 1914, Waves of Sand and Snow and the Eddies That Make Them: Unwin, London, 383 pp.

Costello, W.R., 1974, Development of bed configurations in coarse sand: Experimental Sedimentology Laboratory, Dept. of Earth and Planetary Sciences, MIT, Report 74-1

Eisma, P., 1965, Eolian sorting and roundness of beach and dune sands: Netherlands Jour. Sea Research, 4, 541-555

Ellwood, J.M., Evans, P.D., Wilson, I.G., 1975, Small scale aeolian bedforms: Jour. Sed. Pet., 45, p. 554-561

Ford, E.F., 1957, The transport of sand by wind: Amer. Geoph. Union, Trans., 38, p. 171-174

Gust, G., Southard, J.B., 1980: Breakdown of the universal law of the wall in smooth turbulent flow with weak bed load: In press, 46 pp.

Horikawa, K., Shen, H.W., 1960, Sand movement by wind: Beach Erosion Board, Tech, Memorandum No. 119, 51 pp.

Howard, A.D., 1977, Effects of slope on the threshold of motion and its application to orientation of wind ripples: Geol. Soc. Amer. Bull., 88, p. 853-856

Hsu, S., 1974, Wind stress criteria in eolian sand transport: Jour. Geoph. Res., 76, p. 8684-8688

Hunter, R.E., 1977, Basic types of stratification in small eolian dunes: Sedimentology, 24, p. 361-387

Hussain, A.K.M.F., Reynolds, W.C., 1975, Measurements in fully developed turbulent channel flow: A.S.M.E. Trans., Jour of Fluids Engineering, 97, p. 568-580

Kawamura, R., 1951, Study on sand movement by wind: Reports of the Inst. of Sci. and Tech., Univ. of Tokyo, 5, no. 3-4, Translated: Inst. of Eng. Res., Tech. Report HEL-2-8, Berkeley Ca. (1964), 58 pp.

Kennedy, J.F., 1964, The formation of sediment ripples in closed rectangular conduits and in the desert: Jour. Geoph. Res., 69, p. 1517-1524

Kennedy, J.F., 1969, The formation of sediment ripples, dunes, and antidunes: Annual Rev. of Fluid Mech., 1 p. 147-168

Leatherman, S.P., 1978, A new eolian sand trap design: Sedimentology, 28, p. 303-306

Mattox, R.B., 1955, Eolian shape sorting: Jour. Sed. Pet., 25, p. 133-136

Middleton, G.V., Southard, J.B., 1977, Mechanics of sediment transport: Soc. Econ. Pal. Min. Short Course No. 3, 245 pp.

Miller, M.C., McCave, I.N., Komar, P.D., 1977, Threshold of sediment motion under unidirectional currents: Sedimentology, 24, p. 507-527

Muller, J., 1969, Development of eolian transverse ripples and ripple bedding, Bull. De L'Academic Polonaise Des Sciences, Serie des Sci. Geol. et Geogr., 17, p. 49-56

O'Brien, M.P., Rinlaub, B.D., 1936, The transportation of sand by wind: Civil Engineering, 6, p. 325-327

Owen, R.P., 1964, Saltation of uniform grains in air: Jour. Fluid Mech., 20, p. 225-242

Seppala, M., Linde, K., 1978, Wind tunnel studies of ripple formation: Geografiska Annaler A, 60, p. 29-42

Sharp, R.P., 1963, Wind ripples: Jour. of Geol. 71, p. 617-636

Smith, J.D., 1970, Stability of a sand bed subjected to a shear flow of low Froude number: Jour. Geoph. Res., 75, p. 5928-5940

Southard, J.B., Boguchwal, L.A., Romea, R.D., 1980, Test of scale modelling of sediment transport in steady unidirectional flow: Earth Surface Processes, 5, p. 17-23

Stone, R.O., Summers, H.J., 1972, Study of subaqueous and subaerial sand ripples: Univ. Southern California, Geology Report 72-1

Tanner, W.F., 1966, Ripple mark indices and their uses: Sedimentology, 9, p. 89-104

Tsuchiya, Y., 1970, Successive saltation of a sand grain by wind: Conf. of Coastal Eng. 10, p. 1417-1427

Tsuchiya, Y., 1972, Characteristics of saltation of sand grains by wind: Conf. Coastal Eng. 12, p. 1617-1625

Von Karman, T., 1947, Sand ripples in the desert: Amer. Technion Soc., 6, 52-54

White, B.R., Scholz, J.C., 1977, Magnus effect in saltation: Jour. Fluid Mech., 81, p. 497-512

Willard, B., 1935, An "antidune" phase of eolian ripple marks: Jour. Sed. Pet., 5, p. 133-136

Williams, G., 1963, Some aspects of the eolian saltation load: Sedimentology, 3, p. 257-287

Wilson, I.G., 1971, Aeolian bedforms--their development and origins: Sedimentology, 19, p. 173-210

Wilson, I.G., 1972, Universal dicontinuities in bedforms produced by the wind: Jour. Sed. Pet., 42, p. 667-669

O'Brien, M.P., Rinlaub, B.D., 1936, The transportation of sand by wind: Civil Engineering, 6, p. 325-327

Owen, R.P., 1964, Saltation of uniform grains in air: Jour. Fluid Mech., 20, p. 225-242

Seppala, M., Linde, K., 1978, Wind tunnel studies of ripple formation: Geografiska Annaler A, 60, p. 29-42

Sharp, R.P., 1963, Wind ripples: Jour. of Geol. 71, p. 617-636

Smith, J.D., 1970, Stability of a sand bed subjected to a shear flow of low Froude number: Jour. Geoph. Res., 75, p. 5928-5940

Southard, J.B., Boguchwal, L.A., Romea, R.D., 1980, Test of scale modelling of sediment transport in steady unidirectional flow: Earth Surface Processes, 5, p. 17-23

Stone, R.O., Summers, H.J., 1972, Study of subaqueous and subaerial sand ripples: Univ. Southern California, Geology Report 72-1

Tanner, W.F., 1966, Ripple mark indices and their uses: Sedimentology, 9, p. 89-104

Tsuchiya, Y., 1970, Successive saltation of a sand grain by wind: Conf. of Coastal Eng. 10, p. 1417-1427

Tsuchiya, Y., 1972, Characteristics of saltation of sand grains by wind: Conf. Coastal Eng. 12, p. 1617-1625

Von Karman, T., 1947, Sand ripples in the desert: Amer. Technion Soc., 6, 52-54

White, B.R., Scholz, J.C., 1977, Magnus effect in saltation: Jour. Fluid Mech., 81, p. 497-512

Willard, B., 1935, An "antidune" phase of eolian ripple marks: Jour. Sed. Pet., 5, p. 133-136

Williams, G., 1963, Some aspects of the eolian saltation load: Sedimentology, 3, p. 257-287

Wilson, I.G., 1971, Aeolian bedforms--their development and origins: Sedimentology, 19, p. 173-210

Wilson, I.G., 1972, Universal dicontinuities in bedforms produced by the wind: Jour. Sed. Pet., 42, p. 667-669

Wood, W.H., 1970, Rectification of wind-blown sand: Jour. Sed. Pet., 40, p. 29-37

Zingg, A.W., 1952, A study of the characteristics of sand movement by wind: Unpublished Masters Thesis, Department of Agricultural Engineering, Kansas State Univ. 78 pp.

APPENDIX I

Run Number	Sand	U_{20}(m/s)	U_*(cm/s)	Spacing(cm)	Height(mm)	Ripple Index	Asymmetry Index
1	0.78	8.45	36.6	No morphology data collected			
2	0.78		No data collected				
3	0.78	11.33	60.0	8.81	1.61	54.9	-
4	0.78	10.81	60.0	8.50	1.98	42.9	-
5	0.78	11.58	71.9	9.17	1.05	87.3	0.495
6	0.78	12.48	80.5	Flat-bed transport			
7	0.78	12.88	102.3	Flat-bed transport			
8	0.78	14.21	107.1	Flat-bed transport			
9	0.78	9.50	49.8	7.30	1.92	38.0	0.512
10	0.78	8.38	35.3	6.13	1.28	47.9	0.502
11	0.78	8.66	50.0	6.78	1.60	42.4	0.480
12	0.78		No data collected				
13	0.78	9.78	63.9	7.61	2.01	37.9	0.522
14	0.40	6.84	26.2	Near threshold conditions			
15	0.40	7.22	40.0	4.86	1.31	37.1	0.500
16	0.40	8.26	54.8	5.68	1.18	48.1	0.478
17	0.40	9.25	59.8	5.79	0.76	76.4	0.472
18	0.40	9.88	66.6	7.43	0.75	99.6	0.505
19	0.40	10.51	79.0	Flat-bed transport			
20	0.40		No data collected				
21	0.40	8.66	58.5	5.90	1.16	50.9	0.532

Run Number	Sand	U_{20}(m/s)	U_*(cm/s)	Spacing(cm)	Height(mm)	Ripple Index	Asymmetry Index
22	0.40	7.76	43.2	5.32	1.33	40.0	0.490
23	0.40	9.43	60.2	6.80	0.74	92.4	-
24	0.40	8.92	50.4	5.97	1.06	56.3	-
25	0.40	9.22	53.8	6.37	1.07	59.4	-
26	0.40	9.14	52.3	6.24	1.09	57.2	0.483
27	0.40	9.54	56.1	6.09	1.12	54.4	-
28	0.40	9.50	57.9	6.60	0.61	108.2	0.515
29	0.32	4.91	17.5	Near threshold conditions			
30	0.32	6.12	35.2	4.90	1.44	34.0	0.499
31	0.32	6.99	40.5	5.15	1.41	36.5	0.491
32	0.32	7.72	42.5	5.19	1.32	39.3	0.510
33	0.32	8.38	51.4	6.04	1.26	47.9	0.487
34	0.32	8.96	62.2	6.06	1.04	58.3	0.483
35	0.32	9.71	64.7	6.47	0.76	85.1	0.511
36	0.32	10.79	75.8	Flat-bed transport			
37	0.32	11.21	79.6	Flat-bed transport			
38	0.32	11.71	86.2	Flat-bed transport			
39	0.32	9.40	65.7	6.50	0.88	73.8	-
40	0.32	8.34	57.8	5.92	1.39	42.6	0.500
41	0.32	7.50	44.4	5.50	1.84	30.0	0.518
42	0.32	7.85	53.9	5.71	1.55	36.7	0.505
43	0.32	6.59	37.1	5.26	1.62	32.4	0.502
44	0.32	No data collected					

Run Number	Sand	U_{20}(m/s)	U_*(cm/s)	Spacing(cm)	Height(mm)	Ripple Index	Asymmetry Index
45	0.32	9.50	68.4	6.69	0.95	70.3	0.517
46	0.25	5.90	30.5	5.82	1.93	30.1	0.500
47	0.25	6.28	39.4	5.60	1.89	29.6	0.507
48	0.25	6.89	46.5	6.28	1.75	35.9	0.492
49	0.25	7.58	55.9	6.85	1.94	35.6	0.496
50	0.25	7.76	51.8	7.04	1.45	48.4	0.478
51	0.25	8.50	60.0	7.15	1.62	44.2	0.494
52	0.25	9.07	69.6	7.30	1.23	59.3	0.493
53	0.25	9.36	71.3	7.95	1.59	50.0	0.504
54	0.25	9.50	76.6	8.53	1.03	82.8	0.509
55	0.25	10.25	84.4	Flat-bed transport			
56	0.25	10.08	84.5	Flat-bed transport			
57	0.25	9.85	77.9	9.02	0.98	92.0	0.501
58	0.25	8.26	64.0	7.21	1.51	47.7	0.508
59	0.25	8.77	72.5	7.13	1.19	59.9	0.498
60	0.25	7.13	50.0	6.50	1.70	38.2	0.492
61	0.20	4.33	-	Near threshold conditions			
62	0.20	4.98	31.5	7.23	2.86	25.3	0.506
63	0.20	7.36	44.2	7.99	2.22	36.0	0.477
64	0.20	8.69	52.5	9.45	2.00	47.2	0.497
65	0.20	9.36	57.8	10.57	2.55	41.4	0.479
66	0.20	9.50	62.0	11.28	2.46	45.9	0.460
67	0.20	9.98	69.9	14.41	3.26	44.2	0.480

Run Number	Sand	U_{20}(m/s)	U_*(cm/s)	Spacing(cm)	Height(mm)	Ripple Index	Asymmetry Index
68	0.20	10.85	80.1	15.49	3.25	47.7	0.480
69	0.20	11.21	94.1	18.85	2.25	83.8	0.484
70	0.20	11.54	94.4	23.83	2.89	82.5	0.508
71	0.44	7.50	47.7	9.91	-	-	-
72	0.44	8.92	50.5	8.00	-	-	-
73	0.44	8.22	54.6	7.61	-	-	-
74	0.44	7.45	46.6	7.56	-	-	-
75	0.44	9.43	62.9	8.92	-	-	-
76	0.44	10.72	74.9	7.85	-	-	-
77	0.44	11.42	91.6	7.97	-	-	-
78	0.44	10.22	69.9	10.80	-	-	-